

THE LOCAL VOLUME DATABASE: A LIBRARY OF THE OBSERVED PROPERTIES OF NEARBY DWARF GALAXIES AND STAR CLUSTERS

ANDREW B. PACE^{1,2,*,†}

¹ Department of Astronomy, University of Virginia, 530 McCormick Road, Charlottesville, VA 22904, USA and

² McWilliams Center for Cosmology, Carnegie Mellon University, 5000 Forbes Ave, Pittsburgh, PA 15213, USA

Version November 13, 2024

Abstract

I present the Local Volume Database (LVDB), a catalog of the observed properties of dwarf galaxies and star clusters in the Local Group and Local Volume. The LVDB includes positional, structural, kinematic, chemical, and dynamical parameters for dwarf galaxies and star clusters. I discuss the motivation, structure, construction, and future expansion plans of the LVDB. I highlight catalogs on faint and compact ambiguous Milky Way systems, new Milky Way globular clusters and candidates, and globular clusters in nearby dwarf galaxies. The LVDB is complete for known dwarf galaxies within ~ 3 Mpc and current efforts are underway to expand the database to resolved star systems in the Local Volume. I present publicly available examples and use cases of the LVDB focused on the census and population-level properties of the Local Group and discuss some theoretical avenues. The next decade will be an exciting era for near-field cosmology with many upcoming surveys and facilities, such as the Legacy Survey of Space and Time at the Vera C. Rubin Observatory, the Euclid mission, and the Nancy Grace Roman Space Telescope, that will both discover new dwarf galaxies and star clusters in the Local Volume and characterize known dwarf galaxies and star clusters in more detail than ever before. The LVDB will be continually updated and is built to support and enable future dwarf galaxy and star cluster research in this data-rich era. The LVDB catalogs and package are publicly available as a GitHub repository, `local_volume_database`, and community use and contributions via GitHub are encouraged.

Subject headings: Dwarf galaxies (416), Globular star clusters (656), Astronomy databases (83), Astronomy software (1855)

1. INTRODUCTION

Dwarf galaxies are the most abundant type of galaxy in the universe. The lowest mass dwarf galaxies are among the most chemically pristine and dark matter dominated galaxies known and they are relics from the early universe (e.g., Tolstoy et al. 2009; Frebel & Norris 2015; Simon 2019; Battaglia & Nipoti 2022). They are important probes of galaxy formation, reionization, and stellar feedback on the smallest scales (e.g., Simon 2019; Collins & Read 2022). Only in the Local Group and Local Volume are the lowest mass dwarf galaxies observable and resolved into stars.

Over the past twenty years, the number of low mass dwarf galaxies and stellar systems in the Milky Way (MW), Local Group, and Local Volume has increased exponentially and pushed to fainter and fainter systems (e.g., McConnachie 2012; Müller et al. 2017; Simon 2019; Mutlu-Pakdil et al. 2024). Excitingly, the next generation of upcoming wide-field photometric surveys, such as the Legacy Survey of Space and Time (LSST) at the Vera C. Rubin Observatory, the Euclid mission, and the

Nancy Grace Roman Space Telescope, are on the cusp of starting and they are expected to discover a plethora of new dwarf galaxies (e.g., Hargis et al. 2014; Mutlu-Pakdil et al. 2021). Given the upcoming surveys, an updated census of both the Local Group and Local Volume will assist and enable research into near-field cosmology and nearby dwarf galaxies. In particular, the nearby dwarf galaxies are important cosmological probes to assess the many small-scale issues with our current Λ cold dark matter (Λ CDM) model (e.g., Bullock & Boylan-Kolchin 2017) and to uncover the nature of dark matter (e.g., Buckley & Peter 2018; Tulin & Yu 2018; Strigari 2018; Nadler et al. 2021; McDaniel et al. 2024).

Almost forgotten, there are a number of faint stellar systems in the MW with sizes and luminosities that overlap with the both the faint globular cluster population and faint dwarf galaxy population without a clear classification into their nature (e.g., Cerny et al. 2023a; Smith et al. 2024). There is a renewed interest in these ambiguous systems as some may be the faintest and smallest galaxies (e.g., Manwadkar & Kravtsov 2022), primordial star clusters (Simon et al. 2024), and/or their remnants (e.g., Errani et al. 2024b). Classifying new satellites has been a difficult and time-consuming problem in the MW and classification will only get more difficult with the upcoming surveys. As such, an up-to-date census with the

*pvpacer1@gmail.com or apace@virginia.edu

† Galaxy Evolution and Cosmology (GECO) Fellow

 Github

  ReadTheDocs
Paper Plots

fundamental parameters of known stars clusters will be key to interpret new discoveries.

Here I introduce the Local Volume Database (LVDB), a catalog of nearby dwarf galaxies and star clusters resolved into individual stars. Section 2 lays out the LVDB with subsections on the scope and purpose (§ 2.1), the content, structure, and construction (§ 2.2), how to contribute (§ 2.3), and citations (§ 2.4). Section 3 presents a series of examples and use cases of the LVDB highlighting the content of the LVDB and population level properties of nearby galaxies and star clusters. All examples are publicly available as `jupyter` notebooks on the GitHub repository. Section 4 discusses the current issues and limitations in the LVDB and plans for the expansion of the LVDB. The LVDB is publicly available as a GitHub repository, `local_volume_database`¹.

2. THE LOCAL VOLUME DATABASE

2.1. Scope and Purpose

The primary goals of the LVDB are to: have a complete² catalog of *known* dwarf galaxies and star clusters in the Local Volume, have up-to-date fundamental observed properties of each system with errors and references, be able to easily add newly discovered systems and update any observed property, be able to reference the internal content of the catalog, and enable community contributions. These goals are addressed in the LVDB structure. The LVDB is composed as a collection of YAML³ files, with the properties of an individual system in a single YAML file, which are combined together into user friendly catalogs. Second, the LVDB is hosted as a publicly available GitHub repository.

The LVDB aims to include high-quality measurements of the fundamental properties of both dwarf galaxies and star clusters. While there are existing dwarf galaxy and star cluster catalogs and compilations no database includes both. One key reason to include both types of systems in the LVDB is the large number of existing small and faint systems that are difficult to classify between dwarf galaxies and stars clusters (i.e. ambiguous systems). Furthermore, these systems continue to be discovered in our current surveys. I expect the discovery rate to only increase with upcoming surveys (e.g., LSST).

Here, I refer to the Local Group, the Local Field⁴, and the Local Volume as systems within $d \lesssim 1$ Mpc, within $d \lesssim 3$ Mpc but outside the influence of the MW or M31, and within $d \lesssim 10$ Mpc, respectively. I follow McConnachie (2012) in defining dwarf galaxies as systems fainter than $M_V \sim -18$. While brighter galaxies are included, they are included as “hosts” of the dwarf galaxies or star clusters. Throughout this work, system will refer to a generic object within the LVDB (i.e., both

¹ https://github.com/apace7/local_volume_database

² I note that complete generally refers to whether the LVDB is complete for *known* systems.

³ YAML Ain’t Markup Language

⁴ The edge of Local Group is generally defined at the radius where the local Hubble flow starts and this occurs at $R_{LG} \sim 1$ Mpc (e.g., Karachentsev et al. 2009; Peñarrubia et al. 2014) and the Local Field is commonly defined as Local Group galaxies beyond the MW and M31. Given the catalogs in the LVDB, I define Local Field with an increased distance limit ($d \lesssim 3$ Mpc) as this corresponds to the distance limit that the LVDB is complete for *known* systems.

dwarf galaxies and/or star clusters).

2.2. Content and Structure

The LVDB is a compilation of dwarf galaxies and star clusters and their fundamental observed properties in the nearby universe. The starting point of the dwarf galaxy compilation is the McConnachie (2012) catalog⁵. This has been supplemented by two catalogs: the “Catalog and Atlas of Local Volume galaxies” (Karachentsev et al. 2013)⁶ and the “Extragalactic Distance Database” (Tully et al. 2009; Anand et al. 2021)⁷ and subsequent discoveries. At this point, the LVDB is complete for known dwarf galaxies with $d < 3$ Mpc. The star cluster compilation starts with the Harris (1996) catalog and subsequent discoveries and is supplemented by the more recent measurements compiled in the Galactic Globular Cluster Database⁸ (Baumgardt & Hilker 2018; Baumgardt et al. 2020; Vasiliev & Baumgardt 2021; Baumgardt & Vasiliev 2021). I have chosen not to include stellar streams in this catalog. First, the `galstreams` package⁹ (Mateu 2023) contains an up-to-date list of MW stellar streams and their properties. Second, the properties of stellar streams are more difficult to characterize in the current LVDB structure.

Previous catalogs have used distance ($d \sim 3$ Mpc; McConnachie 2012), membership in the Local Volume with a distance ($d < 12$ Mpc) and/or velocity selection ($v_{LG} < 600 \text{ km s}^{-1}$) (Karachentsev et al. 2013), or type (MW globular cluster or dwarf galaxy) to set their catalog selection. The LVDB selection is to include dwarf galaxies and star clusters that are or can be resolved into individual stars. The effective limit of the LVDB is currently $d \lesssim 10 - 12$ Mpc, however, the dwarf galaxy component is only complete for known systems to 3 Mpc and the LVDB is complete for MW globular clusters and star clusters in nearby dwarf galaxies ($d \lesssim 1$ Mpc). Given that space based telescopes can resolve stars beyond the current LVDB distance limit ($d \sim 10 - 20$ Mpc with the Hubble Space Telescope and beyond $d \sim 40$ with James Webb Space Telescope imaging), I anticipate that the LVDB distance limit will increase in the future.

The LVDB is structured as a collection of YAML files with each system in its own YAML file. The YAML files are then combined into catalogs with additional value-added columns. The measurements compiled in the YAML files include: positions, classification, structural parameters, distance, luminosity, stellar kinematics, stellar chemistry, systemic proper motion, HI gas content, and mean age. The properties and measurements in the input YAML files and the value-added columns are described in detail in Appendix A.

2.2.1. Primary Catalogs

The primary catalogs of the LVDB are split by host and system classification. The primary catalogs are as follows:

⁵ <https://www.cadc-ccda.hia-ihc.nrc-cnrc.gc.ca/en/community/nearby/>

⁶ <https://www.sao.ru/lv/lvgdb/>

⁷ <http://edd.ifa.hawaii.edu/>

⁸ “Fundamental parameters of Galactic globular clusters” <https://people.smp.uq.edu.au/HolgerBaumgardt/globular/>

⁹ <https://github.com/cmateu/galstreams>

- MW dwarf galaxies.
- M31 dwarf galaxies.
- Local Field dwarf galaxies ($d \lesssim 3$ Mpc) unassociated with the MW or M31 (i.e., an updated McConnachie 2012, compilation).
- Local Volume dwarf galaxies ($d \gtrsim 3$ Mpc).
- Ambiguous systems in the MW (generally in the Galactic halo; $|b| \gtrsim 10^\circ$; labeled `gc_ambiguous`). Referred to as ambiguous or hyper-faint¹⁰ compact stellar systems here (HFCSS; see Section 3.9 for a more thorough discussion).
- Globular clusters (GCs) in the Harris (1996) catalog.
- Recently discovered globular clusters (i.e. post-Harris catalog; labeled `gc_mw_new`). These are primarily located at low Galactic latitude ($|b| \lesssim 10 - 20^\circ$) but a few systems are located at high Galactic latitudes. Referred to as GC new or GC new bulge/disk/halo here.
- Globular clusters and star clusters in nearby dwarf galaxies (labeled `gc_dwarf_hosted`). This includes the LMC/SMC globular clusters and star clusters but not any of the globular clusters associated with the Sagittarius dwarf galaxy as they are included in the Harris (1996) catalog. Referred to as GC dwarf hosted here.
- Lower quality candidates, confirmed false positive systems, and background systems. The background systems compiled here were initially considered satellites or members of the Local Volume.

The dwarf galaxy catalogs with $d \lesssim 3$ Mpc are complete for *known* dwarf galaxies. The Local Volume compilation is not complete for known systems and currently focuses on dwarf galaxies that either host globular clusters or are members of one of the closest groups (e.g., Cen A (NGC 5128), NGC 253 (Sculptor), and M 81 (NGC 3031)).

The separation of globular cluster catalogs is based on classification, host, and the common interloper type. The ambiguous systems have a distinct catalog due to their unclear classification between a star cluster or dwarf galaxy. The new Galactic disk/bulge/halo star clusters are split from the Harris catalog as candidates at low Galactic latitude require follow-up spectroscopy to be confirmed due to the higher stellar foreground and open clusters represent an interloper population at low Galactic latitudes. The new Galactic disk/bulge/halo catalog may not be complete for new literature candidates. The dwarf galaxy globular cluster table is not complete and there are many globular cluster candidates that require (spectroscopic) confirmation. Lastly, the candidate/false positive table is not complete and is partly included for any current system in the LVDB that may be classified as a false positive in the future.

¹⁰ I use hyper-faint to refer to $M_V > -3$ (Hargis et al. 2014), although Hargis et al. use $L_V < 10^3 L_\odot$ or $M_V \sim -2.7$ to refer to hyper-faint.

2.2.2. Classification

The LVDB contains two general types of systems (dwarf galaxy and star cluster) and classification is key component of the LVDB. The inclusion of a system in a table has an implicit classification and many systems are not yet confidently classified (generally some combination of faint, small, and/or distant). I follow Willman & Strader (2012) to define a galaxy: “A galaxy is a gravitationally bound collection of stars whose properties cannot be explained by a combination of baryons and Newton’s laws of gravity.” I use the following to define a star cluster: “A star cluster is a self-gravitating bound collection of stars.” There are several classification columns in the LVDB that summarize these definitions.

The following methods are used to classify systems as dwarf galaxies or star clusters:

- dynamical mass-to-light—The gold standard method and most direct method to infer the presence (or absence) of a dark matter halo is to measure the dynamical mass-to-light ratio. For a system with a dark matter halo, the dynamical mass-to-light ratio will be larger than the prediction for a pure stellar system ($\Upsilon_{\text{dyn}} > \text{few} \times \Upsilon_*$). For pressure-supported systems, such as a MW dwarf spheroidal galaxy, this is commonly done by measuring the stellar velocity dispersion from radial velocity of individual stars. For faint systems, the predictions for pure stellar systems are small ($\sigma_* \lesssim 0.1 \text{ km s}^{-1}$) and a dark matter halo is inferred if the velocity dispersion is resolved and non-zero. For low mass systems ($\sigma_v \lesssim 5 \text{ km s}^{-1}$) with small sample sizes ($N \lesssim 20$), the velocity dispersion can be inflated by unresolved binary stars (McConnachie & Côté 2010; Minor et al. 2010, 2019).
- stellar metallicity dispersion—An observed stellar metallicity spread implies the system was able to retain supernova ejecta to self-enrich the next generation of star formation. This indirectly infers the system has or had a dark matter halo to retain the enriched gas (Willman & Strader 2012, and references therein).
- size—Star clusters have smaller sizes ($R_{1/2} \lesssim 10 - 20 \text{ pc}$) than dwarf galaxies and a large size ($R_{1/2} \gtrsim 50 \text{ pc}$) would infer a dwarf galaxy classification. I note that two recently discovered globular clusters, Laevens 1/Crater 1 and Sagittarius II, have relatively large sizes ($R_{1/2} \sim 20 - 30 \text{ pc}$; Weisz et al. 2016; Longeard et al. 2021; Richstein et al. 2024). However, this method stops working for faint luminosities ($M_V \gtrsim -3$), as the star cluster and dwarf galaxy populations overlap in their size distributions.
- mass segregation—The presence of mass segregation in a system can classify a system as a star cluster (e.g., Baumgardt et al. 2022). High mass stars are expected to sink to the centers of the systems and low mass stars pushed to the outskirts. The presence of a dark matter halo significantly increases the timescales for mass segregation (Baumgardt et al. 2022). Old stellar systems with low

relaxation times should be mass segregated (e.g., Forbes & Kroupa 2011; Weatherford et al. 2018, 2020; Baumgardt et al. 2022). Systems with a relaxation time longer than the age of the universe can be classified as galaxies whereas systems with shorter times would be star clusters (Forbes & Kroupa 2011).

- light element abundances—Globular clusters are observed to have light element variations. These variations are generally either correlated (e.g., Na-Ne) or anti-correlated (e.g., Na-O and Mg-Al) (e.g., Carretta et al. 2009). Identifying a system with correlated (or anti-correlated) light element variations can be used to classify a system as a globular cluster. However, the enriched fraction has been found to depend on the initial stellar mass of the globular cluster (e.g., Gratton et al. 2019) and many systems are below this threshold (including all of the ambiguous systems).
- neutron capture elements—Ultra-faint dwarf galaxies and globular clusters are observed to have different abundances of neutron-capture elements (e.g., Sr, Ba, and Eu) (Ji et al. 2019). In general, ultra-faint dwarf galaxies are deficient in neutron-capture elements (Ji et al. 2019) whereas globular clusters follow the MW halo trend. The low neutron-capture elements in ultra-faint dwarf galaxies may be due to stochastic enrichment, metal loss in winds, and short star formation durations (Ji et al. 2019). There are several exceptions to the ultra-faint dwarf galaxy trend which may be evidence for rare enrichment events: Reticulum II (Ji et al. 2016; Roederer et al. 2016), Tucana III (Hansen et al. 2017; Marshall et al. 2019), and Grus II (Hansen et al. 2020).

Lastly, I note that there are some additional types of systems with some ambiguity in their classification: nuclear star clusters, extended clusters, ultra-compact dwarf (galaxies), and tidal dwarf (galaxies). The two former systems are classified here as star cluster here but may contain metallicity spreads or have large sizes and the two latter systems are classified as dwarf galaxies here but may have small sizes or low dynamical masses. See Forbes & Kroupa (2011); Willman & Strader (2012) for more discussion on the classification of these other types of systems.

2.3. Contributions

Community contributions to the LVDB are welcomed and encouraged. While the current content of the LVDB has been collected and curated by myself, community contributions can be easily included by hosting the LVDB as a GitHub repository. Some common anticipated contributions may be adding new systems or adding new measurements of existing systems. In both cases this would consist of adding or editing input YAML files and submitting a GitHub pull request to merge the content into the main branch¹¹. The detailed description of the input YAML files is in Section A and due to the structure

¹¹ This would include validation and confirmation for pull requests by myself or other LVDB GitHub maintainers.

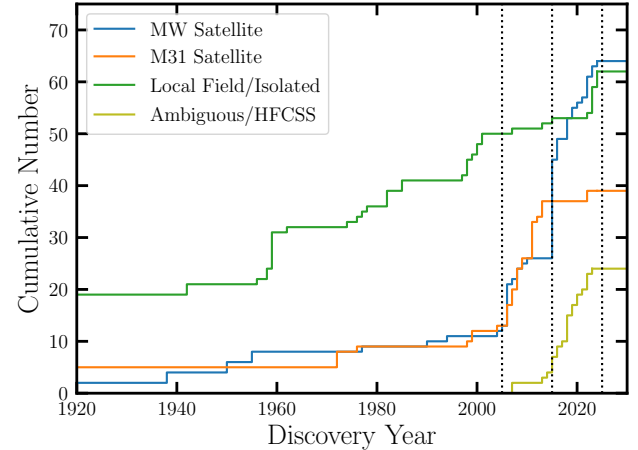


FIG. 1.— The census of dwarf galaxies in the Local Field as a function of discovery year. The cumulative distributions show the number of MW dwarf galaxies (blue), M31 dwarf galaxies (orange), Local Field (green), and ambiguous or hyper-faint compact stellar systems (olive). The three dotted lines at 2005, 2015, 2025 represent the three eras of digital sky surveys: the past SDSS era; the ongoing era with Blanco/DECam, Pan-STARRS, ATLAS, *Gaia*, Subaru/HSC, CFHT/Megacam; the upcoming era with Vera C. Rubin/LSST, Euclid, and Nancy Grace Roman Space Telescope.

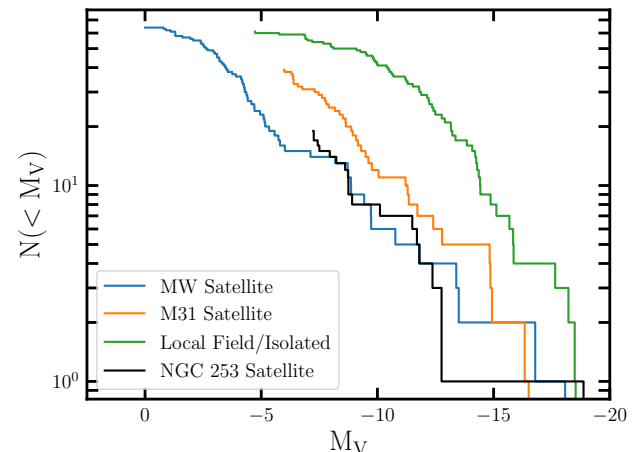


FIG. 2.— The observed cumulative dwarf galaxy luminosity function of the MW (blue), M31 (orange), the Local Field (green), and NGC 253 (black).

of the LVDB, new types of measurements can be added as new YAML keys. Section 4 discusses some current issues and limitations along with a number expansion ideas that are excellent starting areas for anyone interested in contributing.

2.4. Citations

As the LVDB relies on a significant amount of input literature, there are several tools that enable citations to the internal content of the LVDB. Users are encouraged to cite both the LVDB and the internal content used in their analysis. All measurements have the corresponding reference included. The reference columns follow a consistent schema of author last name + Astrophysics

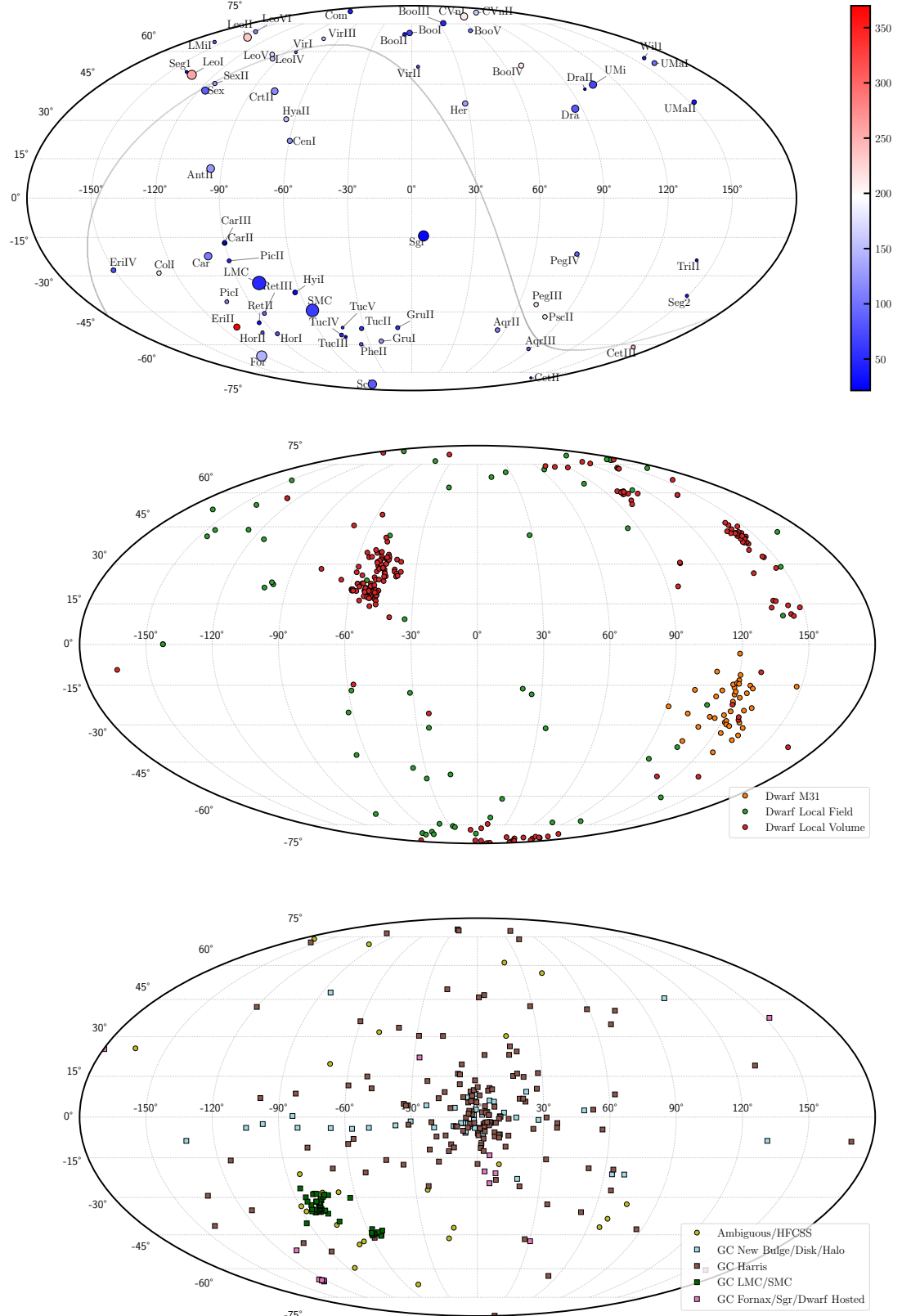


FIG. 3.— Aitoff projection in Galactic coordinates of dwarf galaxies and globular clusters in the LVDB. **Top:** The MW dwarf galaxy population. The size of the points is proportional to the system's stellar mass and the colorbar shows the system's heliocentric distance. Each system is labeled by its abbreviation. For reference, a line is included at $\delta = 0^\circ$. **Middle:** Dwarf galaxies outside the MW including: M31 (orange), Local Field (green), and Local Volume (red). **Bottom:** Milky Way star clusters: ambiguous or HFCSS (olive), globular clusters in the Harris (1996) catalog (brown), newly discovered globular clusters or candidates (light blue), LMC/SMC star clusters (dark green), and star clusters in dwarf galaxies including star clusters associated with the Fornax and Sagittarius dwarf galaxies (pink).

Data System (ADS) bibcode¹². The author’s last name is stripped of special characters and spaces but capitalization is kept. While the ADS bibcode is a unique identifier for a reference, the addition of the author’s last name significantly improves the human interpretability of the LVDB reference schema. To aid in enabling references to the internal contents of the database, there is an up-to-date **BibTeX** file containing all entries in the LVDB with the LVDB reference schema¹³ and there is an ADS library with LVDB references¹⁴. As the ADS bibcode has a fixed length of 19 characters, the ADS bibcode can be derived from the last 19 characters of the LVDB reference schema. There are several **jupyter** notebooks that show examples and assist with LVDB internal citations.

Lastly, users should consider acknowledging the other catalogs and databases that the LVDB was built off of. For dwarf galaxies, this includes the McConnachie (2012) catalog, the “Catalog and Atlas of Local Volume galaxies” (Karachentsev et al. 2013), and the “Extragalactic Distance Database” (Tully et al. 2009; Anand et al. 2021). For globular clusters this includes: the Harris (1996) catalog, and the Galactic Globular Cluster Database (Baumgardt & Hilker 2018; Baumgardt et al. 2020; Vasiliev & Baumgardt 2021; Baumgardt & Vasiliev 2021).

3. USE CASES: THE PROPERTIES OF DWARF GALAXIES AND STAR CLUSTERS IN THE LOCAL GROUP AND BEYOND

To show the content of the LVDB and what it can be used for, I present a series of use cases and examples. **jupyter** notebooks that produce the all of the figures are publicly available in the LVDB GitHub repository¹⁵.

3.1. *Discovery and Census*

The number of dwarf galaxies in the Local Volume has significantly expanded since the start of large digital sky surveys. Figure 1 shows the number of known or candidate dwarf galaxies as a function of time for the MW, M31, Local Field, and the ambiguous/HFCSS MW systems. For MW dwarf galaxies, each generation of sky surveys has roughly doubled the number of known satellites and the next generation of surveys is on the cusp of starting. The initial set of MW dwarf galaxies were discovered on photographic plates¹⁶ (these systems are commonly referred to as the ‘classical’ dwarf spheroidal galaxies) and only the highest surface brightness dwarf galaxies were discovered (e.g., Shapley 1938; Harrington & Wilson 1950; Irwin et al. 1990). With the advent of digital CCDs and the start of the Sloan Digital Sky Survey (SDSS), the number of known dwarf galaxies roughly doubled (from 11 to 26) and the discovery space was pushed into the ultra-faint regime¹⁷ (e.g., Willman et al. 2005; Walsh et al. 2007; Belokurov et al. 2007, 2010). The next generation of wide field surveys (what I refer

to as the current era here) has increased the number of dwarf galaxies to at least 65. This era has been driven by several new instruments on existing telescopes including: DECam on the Blanco telescope, the Panoramic Survey Telescope and Rapid Response System (Pan-STARRS), and the Hyper Suprime-Cam on the Subaru telescope. DECam has been utilized in multiple surveys that have been used to discover new MW satellites such as the Dark Energy Survey (DES; e.g., Bechtol et al. 2015; Drlica-Wagner et al. 2015), the DECam Local Volume Exploration Survey (DELVE; e.g., Mau et al. 2020; Cerny et al. 2023a), and several smaller programs (e.g., Kim et al. 2015; Torrealba et al. 2018). The initial Pan-STARRS survey found several new systems (e.g., Laevens et al. 2014, 2015), and is now part of the Ultraviolet Near Infrared Optical Northern Survey (UNIONS; Smith et al. 2023, 2024). Lastly, the Hyper Suprime-Cam Subaru Strategic Survey was used to discover several new MW satellites (e.g., Homma et al. 2019, 2024) and its data quality is a preview of the data quality in the upcoming LSST.

The Milky Way dwarf galaxy census is now partly limited by the ability to classify faint satellites and there are over 30 satellites without a secure classification. The number of the ambiguous systems or HFCSS has grown in recent years due to sensitive wide-field surveys. Due to the structure of the LVDB, the current ambiguous systems will move to different catalogs when they are confidently classified.

Similarly, the initial M31 satellite dwarf galaxies were discovered on photographic plates (e.g., van den Bergh 1972; Armandroff et al. 1998; Karachentsev & Karachentseva 1999). The M31 dwarf galaxy population has since benefited from all sky surveys such as: SDSS (e.g., Zucker et al. 2004; Bell et al. 2011), Pan-STARRS (Martin et al. 2013a,b), and The Dark Energy Camera Legacy Survey (DECaLS; Collins et al. 2022; Martínez-Delgado et al. 2022). Dedicated deep, wide field surveys such as the Pan-Andromeda Archaeological Survey (PandAS) with CFHT/Megacam has discovered a number of M31 satellites (e.g., Martin et al. 2006; Ibata et al. 2007; Richardson et al. 2011). Many more satellite dwarf galaxies are predicted to exist in the M31 system (Doliva-Dolinsky et al. 2023) but M31 is outside the LSST and Euclid footprints.

While the current surveys have yet to build a complete census of dwarf galaxies within their reach, the next generation of wide-field surveys is about to begin. The first data release of the 10-year LSST at the Vera C. Rubin Observatory is planned for 2026. There are multiple projections for the total MW dwarf galaxy population to be $N \gtrsim 100 - 200$ (e.g., Hargis et al. 2014; Newton et al. 2018; Manwadkar & Kravtsov 2022; Nadler et al. 2024; Ahvazi et al. 2024) and LSST is expected significantly increase number of known MW dwarf galaxies in its footprint. The Euclid mission launched on July 1, 2023 and the first data release is scheduled for 2026 and the Nancy Grace Roman Space Telescope is planned to launch between Oct 2026 to May 2027. While both space telescopes can assist in the MW dwarf galaxy census, their new and unique discovery regime with resolved stars will be low mass dwarf galaxies in the Local Volume (for example, Euclid has already discovered a dwarf galaxy around the MW-analog, NGC 6744 at $d \sim 9.5$ Mpc; Hunt

¹² <https://ui.adsabs.harvard.edu/help/actions/bibcode>

¹³ https://github.com/apace7/local_volume_database/blob/main/table/lvdb.bib

¹⁴ <https://ui.adsabs.harvard.edu/public-libraries/fVKkEJbdRyCmscCOwzsZ6w>

¹⁵ https://github.com/apace7/local_volume_database/tree/main/paper_examples/

¹⁶ This excludes the LMC and SMC which can be seen by eye.

¹⁷ Defined as $M_V > -7.7$ following Simon (2019).

et al. 2024).

Figure 2 shows the observed cumulative luminosity function of dwarf galaxies in the MW, M31, Local Field, and NGC 253¹⁸ systems. Beyond the MW, dwarf galaxy discoveries are just hitting the ultra-faint regime and the next generation of surveys and telescopes (e.g., Rubin/LSST, Euclid, Roman Space Telescope) will have the sensitivity to probe this dwarf galaxy regime. Already, the LVDB is starting to add the dwarf galaxy populations of MW-like systems in the Local Volume (e.g., Cen A, NGC 253, M81, M101).

The dwarf galaxy luminosity function is a key observable in near-field cosmology that probes both the nature of dark matter and galaxy formation physics at low halo masses. Initial research focused on the total number of satellites and whether the number of MW satellite dwarf galaxies was consistent with Λ CDM predictions (e.g., Klypin et al. 1999; Moore et al. 1999; Koposov et al. 2008; Tollerud et al. 2008). More recent studies have shown that the total number is consistent with Λ CDM predictions (Kim et al. 2018), used the dwarf galaxy population to study the minimum halo mass that can host galaxy (Nadler et al. 2020), and placed constraints on different dark matter models (Nadler et al. 2021). Similarly, the satellite luminosity function of other MW-like hosts such as M31 (Doliva-Dolinsky et al. 2023) and Centaurus A (Weerasooriya et al. 2024) can be used to study galaxy formation physics and test environmental differences for MW-like hosts throughout the Local Volume.

3.2. Spatial Distribution

The top panel of Figure 3 shows Aitoff projections in Galactic coordinates of the MW dwarf galaxy satellites. There are a number of spatial alignments and combined with the systemic motion (velocity and proper motion), the phase-space properties of the satellite system can be studied (e.g., Pawłowski 2021). There is a clear overdensity of dwarf galaxies around LMC and SMC in Figure 3. This is the closest example of group infall and a number of satellites have been identified that are or were associated with the LMC and/or SMC (e.g., Kallivayalil et al. 2018; Erkal et al. 2020; Patel et al. 2020; Correa Magnus & Vasiliev 2022; Pace et al. 2022). Other examples of spatial alignments are the candidate Crater-Leo group (Leo II, Leo IV, Leo V, and Crater I; Torrealba et al. 2016; Fritz et al. 2018; Júlio et al. 2024), the vast polar structure (e.g., Lynden-Bell 1976; Pawłowski & Kroupa 2020; Pawłowski 2021), and satellite pairs (e.g., Draco-Ursa Minor, Pisces II-Pegasus III, Carina II-Carina III, Leo IV-Leo V). All the spatial structure in the MW satellite population has the caveat that there are large selection effects along the Galactic Plane.

The central panel of Figure 3 shows Aitoff projections in Galactic coordinates of all the dwarf galaxies in the LVDB beyond the MW. There are several overdensities that correspond to the satellite systems of M31, NGC 253 (Sculptor), Centaurus A (NGC 5128), and M 81 (NGC 3031). Many new dwarf galaxies and candidates have been recently uncovered around NGC 253 (Sand et al. 2014; Martinez-Delgado et al. 2024) and Centaurus A

¹⁸ Of the MW-like galaxies beyond $d > 3$ Mpc, NGC 253 is the only host in the LVDB that is complete for its known satellite galaxy population.

(Crnojević et al. 2014; Müller et al. 2017) due to dedicated deep imaging campaigns and all sky surveys (e.g., DECaLS). The Local Field and Local Volume are areas where upcoming surveys such as Rubin/LSST, Euclid, and Roman will enable the discovery of faint and distant dwarf galaxies (e.g., Mutlu-Pakdil et al. 2021).

The bottom panel of Figure 3 shows the globular and star cluster population of the MW including globular clusters hosted by MW dwarf galaxy satellites (e.g. LMC, SMC, Fornax, Sagittarius). There are many new confirmed and candidate globular clusters at low Galactic latitudes that have been discovered with near-infrared surveys (e.g., Minniti et al. 2011; Garro et al. 2020) and/or with *Gaia* astrometry (e.g., Gran et al. 2022; Pace et al. 2023). Over 30 new confirmed or candidate globular clusters have been uncovered in the Galactic bulge in recent years (Bica et al. 2024; Garro et al. 2024). Since the start of wide-field imaging surveys targeting high Galactic latitude, there are a number of new compact stellar systems in the Galactic halo and while some are clearly star clusters (e.g., Laevens 1/Crater I and Sagittarius II; Weisz et al. 2016; Longeard et al. 2021) the majority are not confidently classified (e.g., Koposov et al. 2007; Cerny et al. 2023a). Several of the HFCSS are likely associated with the LMC and/or SMC (e.g., Martin et al. 2016; Gatto et al. 2021; Cerny et al. 2023b). I note that the LVDB is only complete for old LMC and SMC star clusters. While the population of bright globular clusters at high Galactic latitude ($|b| > 10^\circ$) is generally thought to be complete, the orbital configuration of the current globular clusters suggest there may be 1-3 missing globular clusters in the outer halo (Webb & Carlberg 2021).

Figure 4 shows the Local Volume dwarf galaxies in supergalactic coordinates. The systems are separated by whether they are a satellite or isolated. As the LVDB is not yet complete for distant Local Volume galaxies, the Supergalactic plane does not stand out.

3.3. Systemic Motion and Membership

(Simon 2018)

The systemic motion (v_{los} , $\mu_{\alpha*}$, μ_{δ}) of dwarf galaxies and star clusters is key for membership, associations, and to explore the full phase-space. Figure 5 shows the distance versus velocity for MW and M31 dwarf galaxies. The total velocity can be computed for the majority of the MW dwarf galaxies as systemic proper motions have been measured with *Gaia* astrometry (e.g., Simon 2018; Fritz et al. 2018; McConnachie & Venn 2020; Battaglia et al. 2022; Pace et al. 2022), whereas systemic proper motion measurements exist for only a handful of systems from Hubble Space Telescope (HST) astrometry for M31 dwarf galaxies (e.g., Brunthaler et al. 2007; Sohn et al. 2020; Warfield et al. 2023). For the MW, I include examples with both the total velocity and the corrected Galactocentric radial velocity. The corrected velocity includes a factor of $\sqrt{3}$ to account for the ‘unknown’ tangential velocity and it is included for the MW to show a pre-*Gaia* version. This is a reasonable approximation for the MW and this correction has to be used for almost all other MW-like systems (M31 is the only exception). For some distant MW systems with large proper motion errors, the tangential velocity may be biased to larger values beyond the MW escape velocity (see discussion in

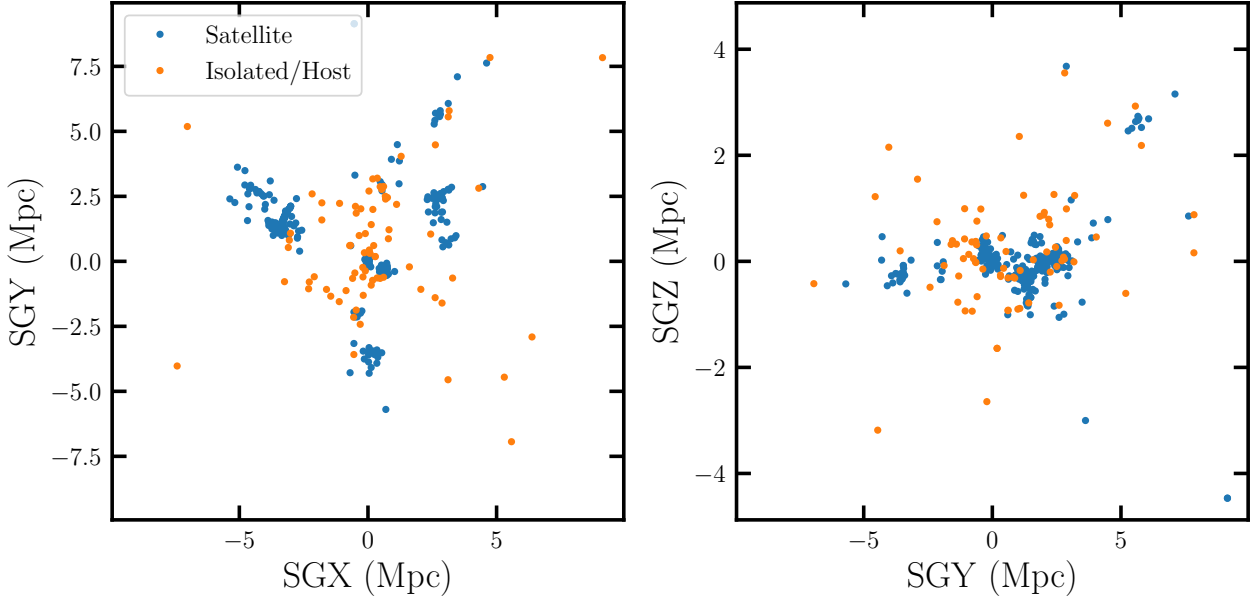


FIG. 4.— The dwarf galaxies in the LVDB in Supergalactic coordinates. The dwarf galaxies are separated by whether they are a satellite (blue) or isolated/host (orange).

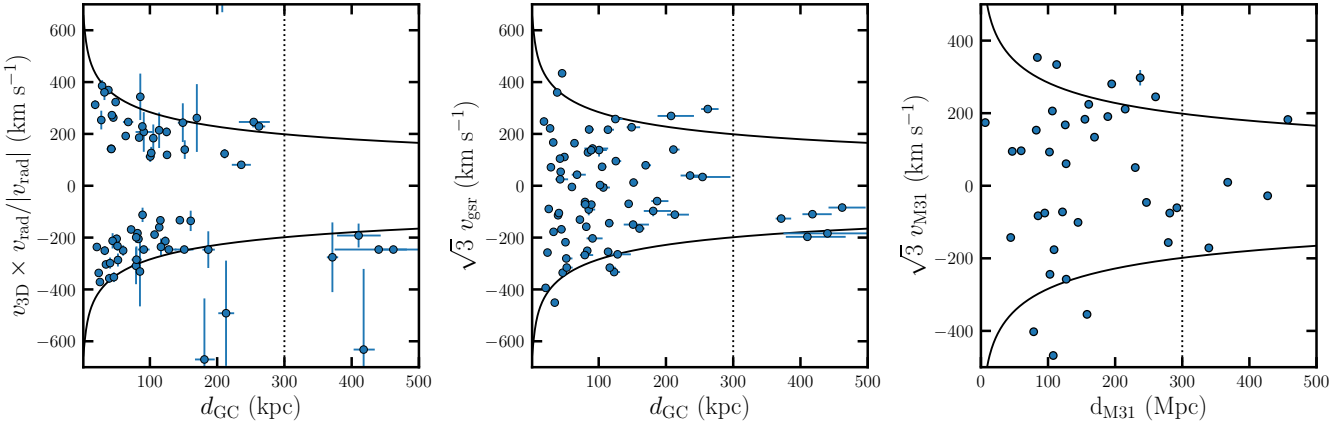


FIG. 5.— Distance versus velocity for the dwarf galaxies in the MW and M31 systems. **Left:** Distance to the Galactic center versus total 3D velocity, where positive (negative) indicates whether the system is moving away from (towards) the Galactic center for MW dwarf galaxies. The solid lines denote the escape velocity curve of the MW with the `MWPotential2014` from `galpy`. The dotted line denotes the approximate virial radius at 300 kpc. **Middle:** Distance to the Galactic center versus corrected Galactocentric velocity for MW dwarf galaxies. A factor of $\sqrt{3}$ is included to account for the tangential velocity and show the approximate total velocity prior to *Gaia* astrometry. **Right:** Velocity and distance relative to M31 for the M31 dwarf galaxies. A similar factor of $\sqrt{3}$ is included to account for the unknown tangential velocity. The same escape velocity and virial radius are assumed for M31 even though more recent mass measurements suggest M31 is more massive than the MW.

van der Marel & Guhathakurta 2008; Correa Magnus & Vasiliev 2022). The last panel of Figure 5 shows the distance versus corrected radial velocity relative to M31 for the M31 dwarf galaxy system. I include escape velocity curves in Figure 5 to estimate membership in MW or M31 system. Full orbit modeling is required to confirm membership and accurate orbital analysis of the MW or M31 needs to the LMC potential (e.g., Erkal & Belokurov 2020; Patel et al. 2020; Pace et al. 2022; Vasiliev 2023) or M33 potential (e.g., Patel et al. 2017; Patel & Mandel 2023), respectively. The LVDB does not include orbital

modeling results for any system but includes the required input measurements.

Figure 6 shows the distance from the Local Group center versus the corrected velocity relative to the Local Group. The Local Group coordinates are computed following Karachentsev & Makarov (1996); Karachentsev et al. (2002) and I assume that the masses of the MW and M31 are equivalent when computing the Local Group coordinates. I include escape velocity curves for a point mass of $5 \times 10^5 M_\odot$ and the local Hubble flow at the zero-velocity surface located at $R_{LG} \sim 1$ Mpc

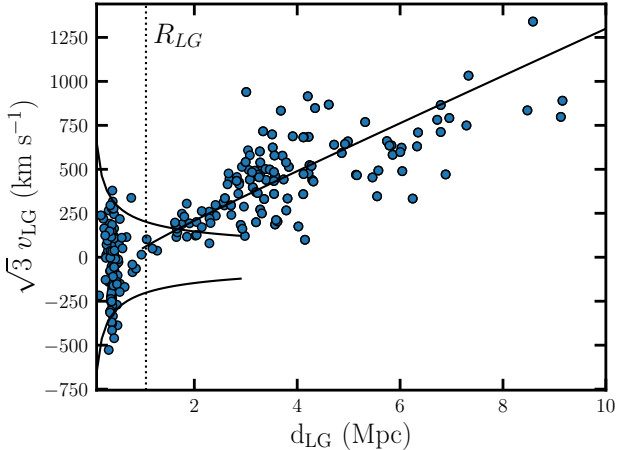


FIG. 6.— Distance versus (corrected) velocity relative to the Local Group for dwarf galaxies in the Local Volume. The solid curves show the escape velocity curves of a point mass with $M_{LG} = 5 \times 10^{12} M_{\odot}$ and are cut off at 3 Mpc. The dotted line is the Local Group turnaround radius, $R_{LG} \sim 1$ Mpc (Karachentsev et al. 2009). The solid line shows the local Hubble flow starting at the Local Group turnaround radius.

(Lynden-Bell 1981; Karachentsev et al. 2009; Peñarrubia et al. 2014). Galaxies within R_{LG} are bound to the Local Group whereas galaxies beyond R_{LG} follow the local Hubble flow (Karachentsev et al. 2009). A handful of systems have systemic proper motion measurements in the Local Group (e.g., Sohn et al. 2020; McConnachie et al. 2021; Battaglia et al. 2022; Bennet et al. 2024) and additional measurements will be possible in the future with long baselines on current or upcoming space based telescopes (e.g., van der Marel et al. 2014; Kallivayalil et al. 2015). The velocity relative to the MW, M31, and Local Group are included in the LVDB catalogs as value-added columns.

3.4. Structure and Luminosity

Figure 7 shows the size-luminosity plane and distance-luminosity plane of dwarf galaxies and star clusters in the MW system. For the characteristic size of each system, I utilize the azimuthally-averaged half-light radius (also known as the geometric mean), defined as $R_{1/2} = R_h \sqrt{1 - \epsilon}$, where R_h is the half-light radius along the major axis and ϵ is the ellipticity. Both latter quantities are compiled as input to the LVDB and $R_{1/2}$ is included as a value-added column. I use the azimuthally-averaged half-light radius to approximate spherical symmetry as most dwarf galaxies are non-spherical. Prior to the discovery of the ultra-faint dwarf galaxies, there was a clear difference in size between globular clusters and dwarf galaxies with dwarf galaxies above $R_{1/2} \gtrsim 100$ pc and globular clusters below $R_{1/2} \lesssim 20$ pc. With over 50 new dwarf galaxies, 20 new globular clusters, and 20 HFCSS, there is now overlap in the size-luminosity plane between different types of systems, especially for $R_{1/2} \lesssim 30$ pc and $M_V \gtrsim -4$. The region with $M_V > -4$ and $15 < R_{1/2} < 25$ pc has been referred to as the “Trough of Uncertainty” due to the overlap of star cluster and dwarf galaxies and the difficulty of classifying

satellites in this region (Conn et al. 2018).

Figure 8 shows the size-luminosity plane for the dwarf galaxy population in the Local Volume. In general, there is broad agreement in size-luminosity distribution of MW, M31, Local Field, and Local Volume dwarf galaxies with the caveat that the closer satellite populations contain fainter dwarf galaxies. There are only a few known dwarf galaxies in the ultra-faint region outside the MW. This includes ~ 10 M31 dwarf galaxies and ~ 5 galaxies in the Local Field (Leo K, Leo M, Peg W, Tuc B; Sand et al. 2022; McQuinn et al. 2023, 2024). The ultra-faint dwarf galaxy region is a promising area of discovery space in the upcoming Rubin/LSST, Euclid, and Roman era for more distant MW-like galaxies (e.g., Mutlu-Pakdil et al. 2021; Hunt et al. 2024).

Structural parameter measurements for nearby systems are commonly determined with individual stars (e.g., Martin et al. 2008; Bechtol et al. 2015) whereas the structural parameters of more distant galaxies are commonly determined with integrated light (e.g., Müller et al. 2017). Though space based imaging (e.g., HST) can resolve stars of the distant dwarf galaxies in the Local Volume (e.g., Mutlu-Pakdil et al. 2024) and analyze the same type of data to determine structural parameters, it has not been done for many systems. Given the different methods, there may be some systematics in the structural parameters between near (resolved stars) and far (integrated light) dwarf galaxies in the Local Volume. Many studies (especially discovery analyses) utilize single parameter density profiles (e.g., Plummer and Exponential profiles) and more luminous systems have been found to be better fit with two-parameter profiles (e.g., Muñoz et al. 2018). While multiple structural profile parameterizations can be included in the LVDB, most systems only have a single parameterization included.

3.5. Stellar Dynamics

The stellar dynamical properties of dwarf galaxies in the Local Field are summarized in Figure 9. The top-left and top-middle panels of Figure 9 compare the velocity dispersion to the stellar size and luminosity. For a pressure-supported system (i.e., a dwarf spheroidal galaxy), the dynamical mass can be computed from the stellar velocity dispersion (e.g., Battaglia & Nipoti 2022). While no results from detailed dynamical models are included in the LVDB, the estimated dynamical mass ($M_{1/2} = M(r = r_{1/2})$) within the 3D deprojected half-light radius¹⁹ ($r_{1/2}$) is computed from the velocity dispersion using the Wolf et al. (2010) mass estimator²⁰. The dynamical mass is compared to the stellar size and luminosity in bottom-left and bottom-middle panels of Figure 9. The top-right and bottom-right panels compare the average density within the 3D half-light radius and the dynamical mass-to-light ratio to luminosity. The dwarf galaxies of the Local Group are among the most dark matter dominated systems in the local universe and are excellent tracers to probe the nature of dark matter (e.g., Gilmore et al. 2007; Chen et al. 2017; Valli & Yu

¹⁹ For many commonly used stellar profiles, the 3D deprojected half-light radius is roughly proportional to the 2D projected half-light radius, $r_{1/2} \sim 4/3 R_{1/2}$ (Wolf et al. 2010).

²⁰ See Walker et al. (2009b); Errani et al. (2018) for other mass estimators.

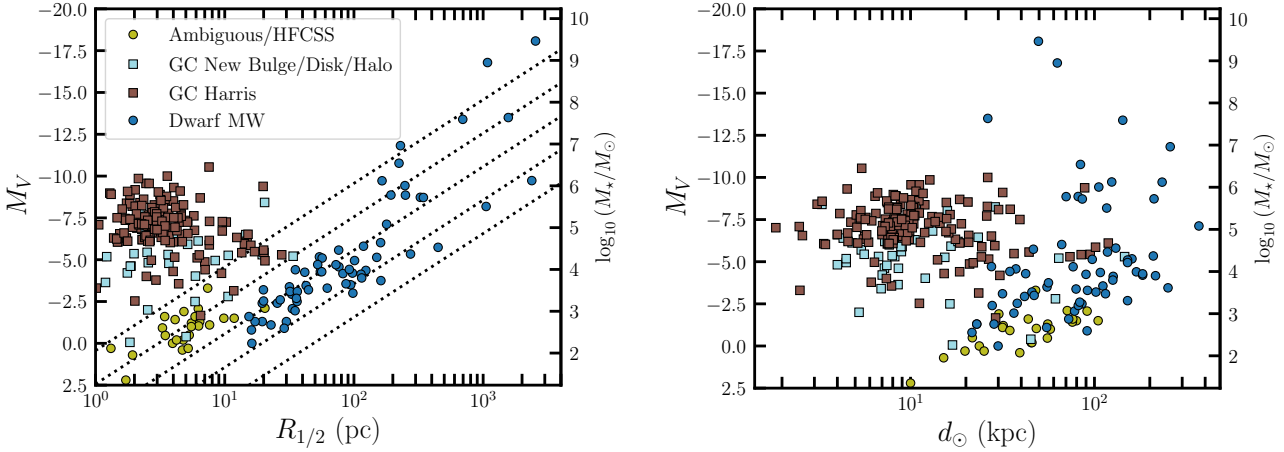


FIG. 7.— **Left:** Azimuthally-averaged half-light radius ($R_{1/2}$) versus absolute V-band magnitude (M_V) and logarithmic stellar mass (M_\star) assuming a mass-to-light ratio of 2 for the MW population of dwarf galaxies (blue), classical globular clusters (brown), new or candidate globular clusters (light blue), and ambiguous or hyper-faint compact stellar systems (olive). **Right:** Heliocentric distance (d) versus absolute V-band magnitude and logarithmic stellar mass for the same systems.

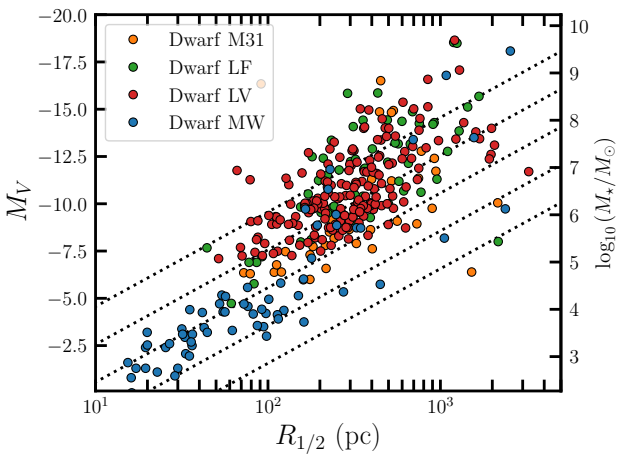


FIG. 8.— Azimuthally-averaged half-light radius ($R_{1/2}$) versus absolute V-band magnitude (M_V) and logarithmic stellar mass (M_\star) for MW (blue), M31 (orange), Local Field (green), and Local Volume (red) dwarf galaxies.

2018; Kim & Peter 2021; Hayashi et al. 2021; Dalal & Kravtsov 2022).

The internal dynamics of dwarf galaxies and star clusters of nearby systems ($d \lesssim 1$ Mpc) are generally measured with radial velocities of individual stars. Due to the faintness of individual stars, this requires multi-object spectroscopy with 8-m class telescopes. Sample sizes range from a several hundreds to a couple thousand in classical satellites (e.g., Walker et al. 2009a; Fabrizio et al. 2016; Pace et al. 2020; Walker et al. 2023) and from tens to almost a hundred stars in ultra-faint dwarf galaxies (e.g., Simon & Geha 2007; Martin et al. 2007; Koposov et al. 2015; Jenkins et al. 2021; Walker et al. 2023; Heiger et al. 2024). These studies commonly target either the Calcium triplet (e.g., Tolstoy

et al. 2023) or Magnesium triplet (e.g., Walker et al. 2023) absorption features for precise and accurate radial velocities. While radial velocities of individual star can be obtained for some nearby Local Field galaxies (e.g., Kirby et al. 2014), going to larger distances requires utilizing Integral Field Unit spectroscopy (e.g., VLT/MUSE, KECK/KCWI; Danieli et al. 2019; Fahrion et al. 2020; Müller et al. 2021), the James Webb Space Telescope (JWST; e.g., Nidever et al. 2024), or future 30m class telescopes.

For ultra-faint dwarf galaxies, one difficult systematic is unresolved binary stars. Systems with the smallest intrinsic velocity dispersion ($\sigma_{\text{los}} \lesssim 5 \text{ km s}^{-1}$), with small spectroscopic sample sizes ($N \lesssim 10 - 20$), and/or without multi-epoch spectroscopic data can have incorrect inferred velocity dispersions if there are unidentified binary stars included. Multiple ultra-faint dwarf galaxies have had their inferred velocity dispersion and dynamical mass reduced after multi-epoch data identified binary stars (e.g., Tri II, Gru I, Her, Tuc II, Boo II; Kirby et al. 2017; Chiti et al. 2022; Ou et al. 2024; Chiti et al. 2023; Bruce et al. 2023). I suspect that some ultra-faint dwarf galaxies with the highest dynamical mass-to-light ratios may contain unidentified binary stars in their current spectroscopic samples and may have inflated dynamical masses.

The stellar kinematics in the LVDB are primarily characterized by the velocity dispersion describing pressure-supported systems. There are some nearby dwarf spheroidal galaxies that are clearly rotating (e.g., And II, Phoenix; Ho et al. 2012; Kacharov et al. 2017) and stellar rotation is not included in the dynamical mass measurements²¹ in Figure 9.

3.6. Stellar Metallicity

²¹ One suggested correction is to replace the velocity dispersion in the mass estimator with a combination of the velocity dispersion and rotation velocity $\sigma_{\text{los}}^2 \rightarrow \sigma_{\text{los}}^2 + (v_{\text{rot}} \sin i)^2$ (Weiner et al. 2006; Kirby et al. 2014)

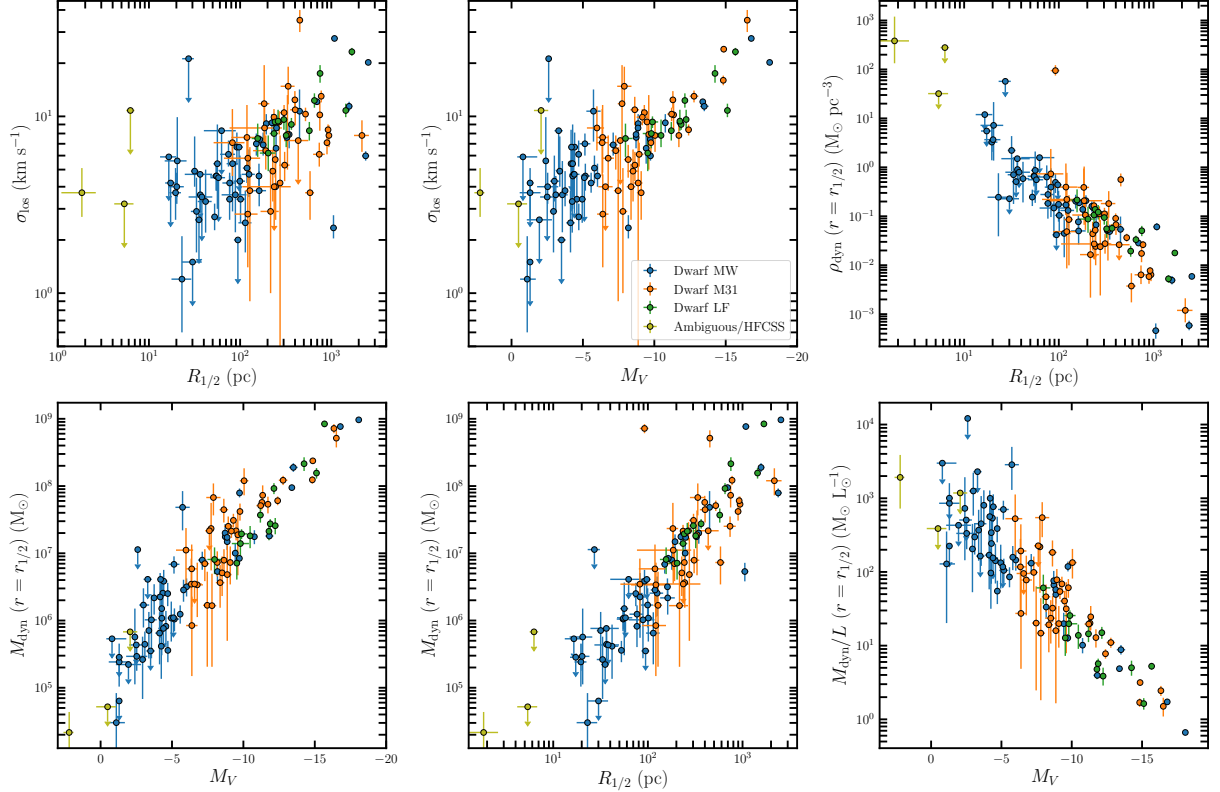


FIG. 9.— The stellar dynamics of nearby dwarf galaxies. **Top-left:** stellar velocity dispersion (σ_{los}) versus projected azimuthally-averaged half-light radius ($R_{1/2}$) for MW dwarf galaxies (blue), M31 dwarf galaxies (orange), Local Field dwarf galaxies (green), and ambiguous or HFCSS (olive). All panels show the same systems. **Top-middle:** stellar velocity dispersion versus absolute V-band magnitude (M_V). **Top-right:** Average density within the 3D half-light radius ($\rho_{\text{dyn}}(r = r_{1/2})$) versus projected azimuthally-averaged half-light radius ($R_{1/2}$). **Bottom-left:** Dynamical mass within the 3D half-light radius ($M_{\text{dyn}}(r = r_{1/2})$) versus absolute V-band magnitude (M_V). **Bottom-middle:** Dynamical mass within the 3D half-light radius ($M_{\text{dyn}}(r = r_{1/2})$) versus azimuthally-averaged projected half-light radius ($R_{1/2}$). **Bottom-right:** Dynamical mass-to-light ratio within the 3D half-light radius versus absolute V-band magnitude (M_V). Note that dynamical mass measurements are made within the 3D half-light radius ($r_{1/2}$) and are compared to the 2D projected half-light radius ($R_{1/2}$). For commonly used stellar density profiles, $r_{1/2} \sim 4/3 R_{1/2}$ (Wolf et al. 2010).

The mean stellar metallicity ([Fe/H]) and metallicity dispersion of dwarf galaxies and globular clusters in the MW system is shown in Figure 10. The LVDB contains metallicity measurements from photometry (e.g., metallicity sensitive photometry), isochrone/color-magnitude diagram fits, and spectroscopic metallicity (either from high or medium resolution spectroscopy). Spectroscopic metallicities are favored over isochrone and photometric metallicity²² for summary measurements in the LVDB and I outline systems with spectroscopic metallicity in Figure 10. While the MW dwarf galaxies display a clear trend with stellar mass and metallicity (i.e., they follow the stellar mass-metallicity relation; Kirby et al. 2013b), there is no obvious trend for the MW globular cluster system. The metallicity dispersion is a useful measurement to distinguish dwarf galaxies from star clusters as dwarf

²² I note that in some cases, much larger samples of metallicity measurements for individual stars can be obtained with metallicity sensitive narrowband photometry (e.g., Ca H&K) compared to spectroscopic samples (e.g., Fu et al. 2023, 2024) and these samples would better describe a system's metallicity distribution than a small spectroscopic sample.

galaxies will have a metallicity spread while star clusters²³ will generally not. Along these lines, there is an observed metallicity floor at [Fe/H] ~ -2.5 in the MW globular clusters system²⁴ and the mean stellar metallicity can be used with the stellar mass-metallicity relation to assist with classification (e.g., Simon et al. 2017).

Figure 11 shows the summary of the mean metallicity and metallicity dispersion for the dwarf galaxies in the Local Volume. For dwarf galaxies in the Local Volume, there is a clear trend between stellar mass and stellar metallicity (Kirby et al. 2013b). The stellar mass-stellar metallicity relation and correlation is used to test chemical evolution models, inflows and outflows, and stellar feedback models (e.g., Garnett 2002; Finlator & Davé 2008; Kravtsov & Manwadkar 2022). There is an observed metallicity plateau at [F/H] ~ -2.6 for the

²³ I note that the LVDB is generally incomplete for existing metallicity dispersion measurements for globular clusters.

²⁴ Although there are two MW globular cluster stellar streams and an M31 globular cluster below the MW metallicity floor (Wan et al. 2020; Larsen et al. 2020; Martin et al. 2022).

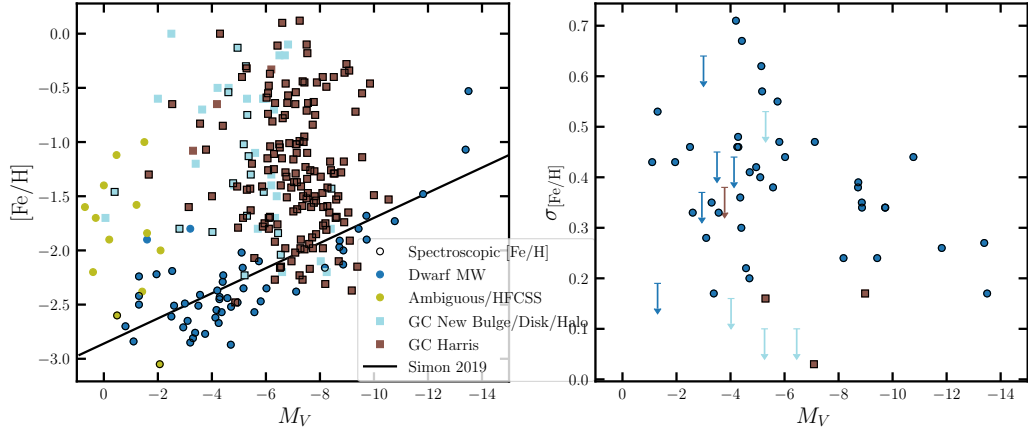


FIG. 10.— **Left:** Absolute V-band magnitude (M_V) versus mean stellar metallicity ($[\text{Fe}/\text{H}]$) for satellites in the MW system including: MW dwarf galaxies (blue), ambiguous or hyper-faint compact stellar systems (olive), new globular clusters in the bulge, disk, and halo (light blue), and globular clusters in the Harris catalog (brown). Systems with spectroscopic metallicities are outlined in black circles and the stellar mass-stellar metallicity relation from Simon (2019) is included. **Right:** Absolute V-band magnitude versus metallicity dispersion ($\sigma_{[\text{Fe}/\text{H}]}$) for the same systems.

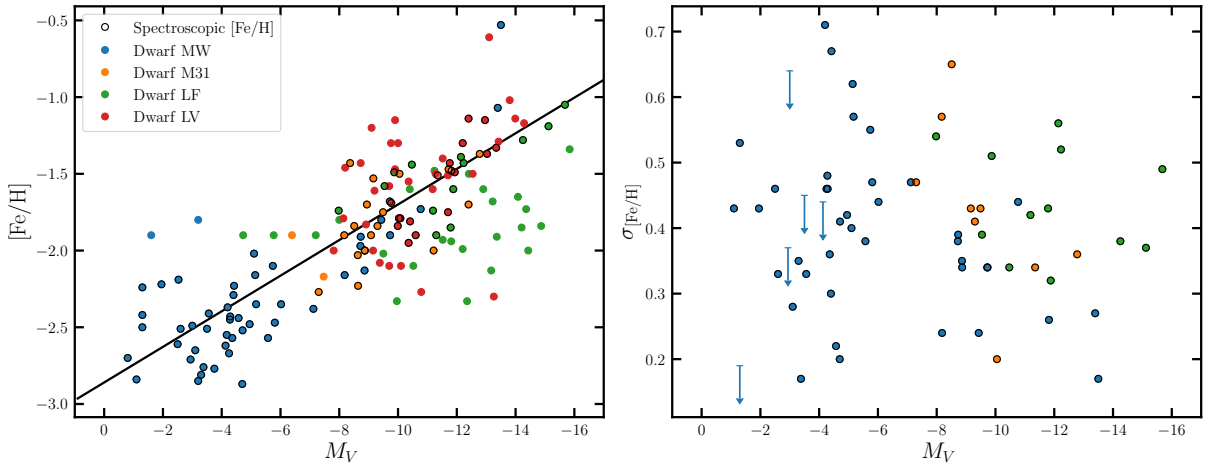


FIG. 11.— **Left:** Absolute V-band magnitude (M_V) versus mean stellar metallicity ($[\text{Fe}/\text{H}]$) for MW (blue), M31 (orange), Local Field (green), and Local Volume (red) dwarf galaxies. Systems with spectroscopic metallicities are outlined in black circles and the stellar mass-stellar metallicity relation from Simon (2019) is included. **Right:** Absolute V-band magnitude versus metallicity dispersion ($\sigma_{[\text{Fe}/\text{H}]}$) for the same systems.

faintest MW dwarf galaxies (Fu et al. 2023). The inclusion of the intergalactic medium metallicity in semi-analytic models can explain the observed metallicity floor (Kravtsov & Manwadkar 2022; Ahvazi et al. 2024). The metallicity dispersion for dwarf galaxies ranges from 0.2–0.7 dex and there is no clear trend with luminosity. Less work has been done to explain the large range in metallicity dispersion and physical processes include the stochasticity of chemical enrichment processes and (inhomogeneous) metal mixing (e.g., Greif et al. 2010; Frebel et al. 2014; Emerick et al. 2020). Understanding the stellar metallicity distribution of dwarf galaxies in the Local Group is key for testing stellar feedback and chemical evolution models.

3.7. Globular Clusters

The LVDB has several globular clusters and star clusters catalogs including: Harris/classical, new bulge/disk/halo, dwarf galaxy hosted, and the ambiguous hyper-faint compact stellar systems. The majority of the globular clusters in the LVDB catalogs are located in MW or its satellites. The only globular clusters beyond the MW are hosted in nearby Local Field or Local Volume dwarf galaxies. The properties of the globular clusters in the LVDB (size, luminosity, metallicity, and age) are summarized in Figure 12. The majority of the globular clusters are bright ($M_V < -5$) but there is a tail to fainter systems. There is a similar tail to larger sizes ($R_{1/2} > 10$ pc). Whether these systems lost their

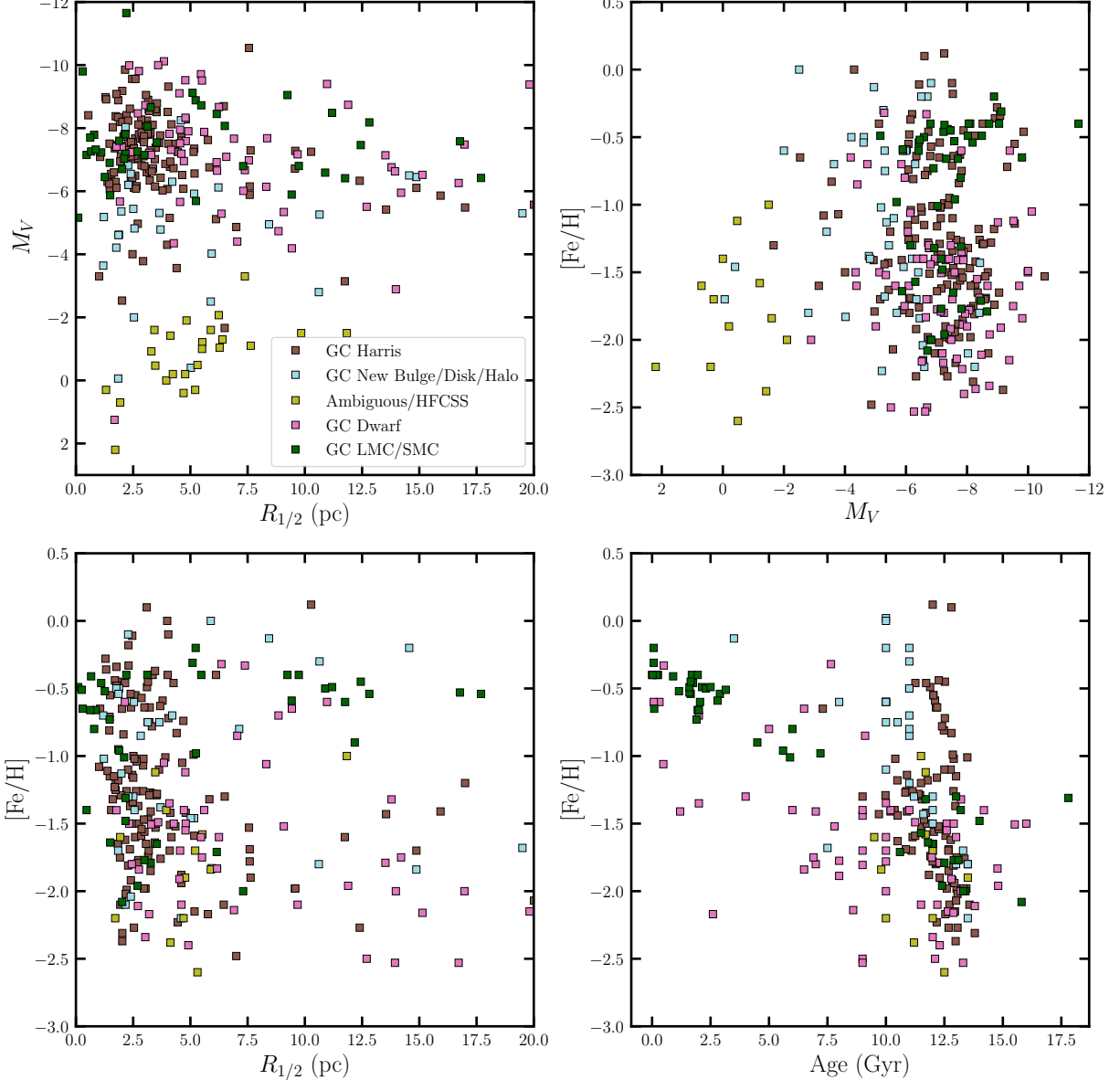


FIG. 12.— Properties of globular clusters and star clusters in the MW system. The systems are the same for all panels and include: classical/Harris (1996) catalog globular clusters (brown), new globular clusters and candidates in Galactic disk, bulge, and halo (light blue), ambiguous or hyper-faint compact stellar systems (olive), star clusters in dwarf galaxies (pink), and LMC/SMC star clusters (dark green). **Top-left:** azimuthally-averaged half-light radii ($R_{1/2}$) versus absolute V-band magnitude (M_V). **Top-right:** absolute V-band magnitude (M_V) versus mean metallicity ([Fe/H]). **Bottom-left:** azimuthally-averaged half-light radii ($R_{1/2}$) versus mean metallicity ([Fe/H]). **Bottom-right:** age versus mean metallicity ([Fe/H]).

stellar mass due to internal dynamical effects or external tidal forces is an open question and likely depends on properties specific to each individual cluster.

While one motivation for the globular cluster compilations in the LVDB is for comparisons to newly discovered stellar systems and assist in classification, there are many new systems that have not been compiled in the literature. This includes the ambiguous systems or hyper-faint compact stellar systems, globular clusters hosted by dwarf galaxies, and the more recently discovered globular

clusters and candidates²⁵. More recently discovered globular clusters are generally fainter ($M_V > -5$) and/or located in regions with higher stellar densities (i.e., Galactic bulge and disk). While the number of bright globular clusters in the MW halo and at higher Galactic latitude is thought to be roughly complete (e.g., Webb & Carlberg 2021) there are many new candidates at low Galactic

²⁵ Although two recent studies have compiled newly discovered globular clusters and candidates in the Galactic bulge (Bica et al. 2024; Garro et al. 2024).

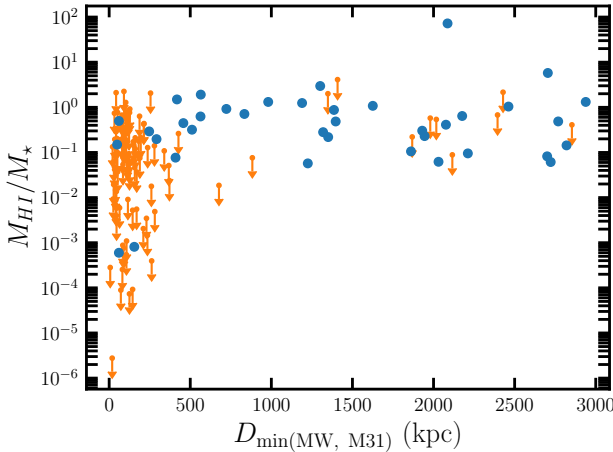


FIG. 13.— Distance to the closest massive galaxy (MW or M31) versus the ratio of HI gas mass to stellar mass versus for dwarf galaxies in the Local Field. The majority of satellites are quenched with the exception of some massive satellites whereas many isolated dwarf galaxies retain their gas reservoir.

latitudes (e.g., Minniti et al. 2011; Gran et al. 2022).

At a population level, the kinematics of globular clusters along with their age and metallicity have been used to understand their origin and connection to accretion events (Massari et al. 2019; Kruijssen et al. 2019). Recent analysis has studied the census of globular clusters and candidates in Galactic bulge and compared the globular cluster metallicity distribution to the in-situ MW stellar populations and ex-situ accretion events (Bica et al. 2024; Garro et al. 2024). Properties such as the number and mass in globular cluster systems correlates with the stellar and halo mass of the host galaxy (e.g., Spitler & Forbes 2009; Forbes et al. 2018; Eadie et al. 2022) and the many dwarf galaxies without globular clusters can still be used to determine these relations (e.g., Berek et al. 2023). The LVDB compilation of globular clusters hosted by dwarf galaxies will be useful for studies on understanding the connection between globular cluster systems and host galaxy properties. In particular, why do some low mass dwarf galaxies host globular clusters while other dwarf galaxies at the same stellar mass do not?

3.8. Neutral Hydrogen Gas

The LVDB includes measurements of the neutral hydrogen gas flux. Figure 13 shows the ratio of HI mass to stellar mass versus the minimum distance to the MW or M31 for Local Field dwarf galaxies. The majority of satellites are quenched except for some massive satellites whereas many isolated dwarf galaxies retain their gas reservoir (e.g., Einasto et al. 1974). There are several environmental processes that can strip the HI gas and quench infalling low mass dwarf galaxies such as ram-pressure stripping and turbulent viscous stripping (e.g., Fillingham et al. 2016). The primary HI property cataloged in the LVDB is the HI flux. One key HI property that is missing in the LVDB are kinematic measurements and their inclusion would increase the number of low mass dwarf galaxies with dynamic mass measurements

(e.g., Oh et al. 2015). A significant number of systemic velocity measurements of distant dwarf galaxies in the LVDB are from HI results.

3.9. Ambiguous or Hyper-Faint Compact Stellar Systems

The ambiguous or hyper-faint compact stellar systems²⁶ (HFCSS) are a category of systems compiled in the LVDB for the first time. One goal of the HFCSS compilation is to encourage the community to study these mostly forgotten systems and assist in classifying them. The HFCSS populate the compact ($R_{1/2} < 10 - 20$ pc) and faint ($M_V > -3$) region of the size-luminosity plane. The HFCSS are located in the region of the size-luminosity plane when both the star cluster or dwarf galaxy populations would be located if extrapolated to fainter magnitudes. This small and faint region has been referred to as the “valley of ambiguity” or the “trough of uncertainty.” Of note, all known systems are located in the Galactic halo and could not be found at low Galactic latitudes due to higher stellar backgrounds. It is unclear whether these systems have undergone extreme tidal disruption (e.g., Errani et al. 2024b). Many of these systems were initially considered star clusters²⁷ based on photometric analysis but the majority lack any spectroscopic follow-up. Compared to when the first HFCSS were discovered, there are now theoretical predictions that hyper-faint dwarf galaxies should exist in the MW to $M_V \sim 0$ (e.g., Manwadkar & Kravtsov 2022).

There are already systems in the dwarf galaxy or globular cluster catalogs that would be considered HFCSS if they lacked spectroscopic follow-up. There are four globular clusters in the Harris catalog, AM 4, Palomar 1, Palomar 13, and 2MASS GC-02, that have sizes and luminosity that are in (or just outside) the HFCSS region. All have spectroscopic follow-up that suggests they are faint globular clusters (e.g., Bradford et al. 2011; Kundler et al. 2021). Similarly, there are several recently discovered star clusters in the HFCSS region, Laevens 3, Muñoz 1, and Segue 3, with spectroscopic follow-up that classifies them as star clusters (Fadely et al. 2011; Muñoz et al. 2012; Longeard et al. 2019). There are several dwarf galaxies in the HFCSS region, Draco II, Triangulum II, Segue 1, Segue 2, Tucana V, and Willman 1, with a metallicity spread and/or a resolved velocity dispersion from spectroscopic follow-up (Kirby et al. 2013a, 2017; Fu et al. 2023; Simon et al. 2011; Hansen et al. 2024; Fu et al. 2023; Willman et al. 2011). Some of these systems may be tidally influenced; for example, Segue 1, Triangulum II, and Willman 1 have orbital pericenters of 20, 12, and 16 kpc, respectively (Pace et al. 2022). At least one system, Tucana III, has no resolved velocity or metallicity dispersion but has been considered a dwarf galaxy due to its size, mean metallicity,

²⁶ I note that these systems have many names in the literature: ultra-faint star clusters, micro galaxies/glofs (Errani et al. 2024a,b), ultra-faint objects (Contenta et al. 2017), ultra-faint compact satellites, ultra-faint compact stellar systems (Circiello et al. 2024), faint ambiguous satellites (Smith et al. 2024), faint halo clusters (Bica et al. 2019), hyper-faint compact stellar systems and/or ambiguous systems (this work). I (and some colleagues) have referred to these systems as ultra-faint star clusters for years which incorrectly suggested a classification for these systems.

²⁷ Almost of these systems follow star cluster naming conventions.

orbit, and tidal disruption (Simon et al. 2017; Li et al. 2018). The Ursa Major III/UNIONS 1 system has a resolved velocity dispersion but the removal of 1-2 potential outlier stars from the measurement leads to an unresolved velocity dispersion and without a metallicity measurement the classification remains unclear (Smith et al. 2024) and I consider it a HFCSS here. The systems, Draco II and Eridanus III, have conflicting classification evidence as there is observed mass segregation in both systems that suggests a star cluster origin (Baumgardt et al. 2022) while both systems also have a resolved metallicity dispersion from metallicity sensitive narrow-band photometry that suggests a dwarf galaxy origin (Fu et al. 2023). The main difference between the two systems is their size and Draco II is currently classified as a galaxy while Eridanus III is considered a HFCSS. I note that several HFCSS have evidence for mass segregation: Kim 2, Kim 3 (Kim et al. 2015, 2016), Balbinot 1, DES 1, Koposov 1, Koposov 2, and Segue 3 (Baumgardt et al. 2022). Even with spectroscopy, the faintest HFCSS may be difficult to classify. Spectroscopy of DELVE 1 and Eridanus III has found the brightest star of both systems to be very metal-poor ($[\text{Fe}/\text{H}] \sim -3.1, -2.8$) and Carbon-enhanced (Simon et al. 2024) but lack spectroscopic metallicity spread constraints due to the lack of stars bright enough of measurements. Carbon-enhanced stars are extremely rare in star clusters.

In summary, the MW contains a number of compact ($R_{1/2} < 20$ pc) and faint ($M_V > -3$) satellites. While some systems with spectroscopic follow-up in this size and luminosity range have been confidently classified as star clusters or dwarf galaxies, the majority lack any spectroscopic follow-up and cannot be classified as dwarf galaxies or star clusters. These systems represent either the extreme faint end of the star cluster population or the extreme faint end of the dwarf galaxy population. Regardless of their classification, the systems may have undergone extreme tidal stripping and they may have tidal tails below current surface brightness limits. The existence of the HFCSS can help identify the minimum halo mass for galaxy formation and/or help understand how some systems survive in tidal fields.

4. ISSUES, LIMITATIONS, EXPANSION, AND FUTURE DEVELOPMENT

There are some current issues and limitations with the LVDB along with many ideas or requests for expanding the LVDB. The current format of the LVDB does not limit the resolution of these issues and enables the expansion of the LVDB for additional properties and measurements. Community feedback, assistance, and contribution will drive the resolutions of these issues and is welcome.

- The current structure of the database was created and optimized for studies of MW dwarf spheroidal galaxies. These systems are all resolved into individual stars and excluding the LMC and SMC, lack HI gas.
- The database includes a variety of techniques and methods for both measurements and analyses. Due to this inhomogeneity, there will be systematics in the LVDB and some studies may opt for homogenized measurements.

- As previously mentioned, many catalogs are currently incomplete for *known* systems in the Local Volume. This includes dwarf galaxies beyond 3 Mpc, LMC/SMC star clusters, and star clusters beyond the MW including dwarf galaxy hosted star clusters. In addition, there are several obvious types of systems such as the M31 globular clusters²⁸ and the MW open clusters²⁹ that are entirely absent from the LVDB.
- When new YAML collections and keys have been added, there has not been a significant effort to populate measurements for existing systems (e.g., type, E(B-V), star formation history/quenching times).
- Many systems are missing discovery references. This is especially true for systems discovered before the start of my academic career.
- Some galaxies show changes in the position angle and/or ellipticity with radius and the current LVDB format does not account for this.
- The current stellar kinematic setup assumes a system has a constant velocity dispersion and no rotation. While this has been traditionally true for MW dwarf spheroidal galaxies (e.g., Walker et al. 2007), some dwarf spheroidal galaxies are clearly rotating (e.g., And II; Ho et al. 2012) and others may contain velocity gradients (e.g., Leo V, Ant II; Collins et al. 2017; Ji et al. 2021).
- The stellar metallicity distribution is based on the mean (or median) and dispersion. Most observed metallicity distributions are generally non-Gaussian and skewed (e.g., Kirby et al. 2011) and most dwarf galaxies have radial metallicity gradients (e.g., Taibi et al. 2022).
- There is existing HI kinematic literature that is not included for many galaxies and there are other HI summary properties that could be included (line width profile measurements or the flat velocity of the rotation curve, v_{flat}).
- There are multiple definitions of the Sersic profile in the literature. While an effort has been made to homogenize these measurements, there may be some inconsistencies.
- There are a number of systems without an independent distance measurement and they inherit the distance and errors of their host galaxy. This is generally globular clusters hosted by dwarf galaxies and distant dwarf galaxy candidates. This is not denoted in the combined catalogs.

²⁸ There are two existing catalogs that summarize the properties of the M31 globular clusters: “The Revised Bologna Catalogue” (<http://www.bo.astro.it/M31/> Galleti et al. 2004) and “Studies of Resolved Objects in M31” https://lweb.cfa.harvard.edu/oir/eg/m31clusters/M31_Hectospec.html.

²⁹ There are several existing catalogs that summarize the census and properties of MW open clusters (e.g., Bica et al. 2019; Cantat-Gaudin & Anders 2020; Hunt & Reffert 2023).

- The LVDB currently only includes V -band magnitude measurements (both apparent and absolute) and it would be beneficial to include magnitudes in both other bands and other photometric systems (UBVI, SDSS, etc).
- The stellar kinematics are based solely of the line-of-sight kinematics. The kinematics from internal tangential motions (i.e., proper motions) are available for many of the closer MW globular clusters from *Gaia* or HST astrometry (e.g., Vasiliev & Baumgardt 2021; Libralato et al. 2022) and several dwarf galaxies (Massari et al. 2018; Vitral et al. 2024). Internal tangential kinematic measurements will be enabled with future long-term astrometric measurements.
- The central surface brightness is not included.
- I have chosen not to include orbital information (pericenter, apocenter, etc). These quantities are dependent on a number of model choices such as the MW potential, LMC inclusion, and/or solar motion.
- There are a number of other observational properties that could be included: RR Lyrae or other variable star summary statistics, gas phase metallicity (O/H), and star formation rates tracers such as the flux in H_{α} , near- and far-UV.

5. SUMMARY

The Local Volume database (LVDB) is a compilation of observed properties of dwarf galaxies and star clusters in the Local Volume. I have presented an overview of the structure and construction of the LVDB and some ideas for future expansion. The LVDB will be useful for comparing new observational results or theoretical models to the dwarf galaxy and star cluster populations in the

Local Volume. I have presented several use cases and examples along with public `jupyter` notebooks. The LVDB is publicly available as a GitHub repository³⁰ and community contributions are encouraged. There are many upcoming surveys, such as the LSST at the Vera C. Rubin Observatory, the Euclid mission, and the Nancy Grace Roman Space Telescope, that will significantly expand our knowledge of the Local Volume and push the frontier of dwarf galaxy and star cluster research. The upcoming era of near-field cosmology is bright and the LVDB is a tool built to enable research for this exciting era.

ACKNOWLEDGEMENTS

I thank Jordan Bruce, Rachel Buttry, Jeff Carlin, William Cerny, Denija Crnojević, Alex Drlica-Wagner, Marla Geha, Alex Ji, Nitya Kallivayalil, Sergey Koposov, Ting S. Li, John Maner, David Nidever, Liam Plybon, Dave Sand, Josh Simon, Louie Strigari, Chin-Yi Tan, Erik Tollerud, Kathy Vivas, Matt Walker, and Brian Yanny for helpful conversations about the LVDB, comments on the draft, and testing initial versions of the LVDB.

ABP acknowledges partial support by NSF grant AST-2206046.

This research has made use of NASA’s Astrophysics Data System Bibliographic Services and the arXiv preprint server. I acknowledge the usage of the HyperLeda database³¹ (Makarov et al. 2014).

SOFTWARE

`astropy` (Astropy Collaboration et al. 2013, 2018), `matplotlib` (Hunter 2007), `NumPy` (Walt et al. 2011), `iPython` (Pérez & Granger 2007), `SciPy` (Virtanen et al. 2020) `corner.py` (Foreman-Mackey 2016), `emcee` (Foreman-Mackey et al. 2013), `gala` (Price-Whelan 2017), `galpy`³² (Bovy 2015),

REFERENCES

Ahvazi N., Benson A., Sales L. V., Nadler E. O., Weerasooriya S., Du X., Bovill M. S., 2024, MNRAS, 529, 3387

Anand G. S., et al., 2021, AJ, 162, 80

Armandroff T. E., Davies J. E., Jacoby G. H., 1998, AJ, 116, 2287

Astropy Collaboration et al., 2013, A&A, 558, A33

Astropy Collaboration et al., 2018, AJ, 156, 123

Battaglia G., Nipoti C., 2022, Nature Astronomy, 6, 659

Battaglia G., Taibi S., Thomas G. F., Fritz T. K., 2022, A&A, 657, A54

Baumgardt H., Hilker M., 2018, MNRAS, 478, 1520

Baumgardt H., Vasiliev E., 2021, MNRAS, 505, 5957

Baumgardt H., Sollima A., Hilker M., 2020, PASA, 37, e046

Baumgardt H., Faller J., Meinhold N., McGovern-Greco C., Hilker M., 2022, MNRAS, 510, 3531

Bechtol K., et al., 2015, ApJ, 807, 50

Bell E. F., Slater C. T., Martin N. F., 2011, ApJ, 742, L15

Belokurov V., et al., 2007, ApJ, 654, 897

Belokurov V., et al., 2010, ApJ, 712, L103

Bennet P., et al., 2024, ApJ, 971, 98

Berek S. C., Reina-Campos M., Eadie G., Sills A., 2023, MNRAS, 525, 1902

Bica E., Pavani D. B., Bonatto C. J., Lima E. F., 2019, AJ, 157, 12

Bica E., Ortolani S., Barbuy B., Oliveira R. A. P., 2024, A&A, 687, A201

Bonnivard V., et al., 2015, MNRAS, 453, 849

Bovy J., 2015, ApJS, 216, 29

Bradford J. D., et al., 2011, ApJ, 743, 167

Bruce J., Li T. S., Pace A. B., Heiger M., Song Y.-Y., Simon J. D., 2023, ApJ, 950, 167

Brunthaler A., Reid M. J., Falcke H., Henkel C., Menten K. M., 2007, A&A, 462, 101

Buckley M. R., Peter A. H. G., 2018, Phys. Rep., 761, 1

Bullock J. S., Boylan-Kolchin M., 2017, ARA&A, 55, 343

Cantat-Gaudin T., Anders F., 2020, A&A, 633, A99

Carretta E., Bragaglia A., Gratton R., Lucatello S., 2009, A&A, 505, 139

Cerny W., et al., 2023a, ApJ, 953, 1

Cerny W., et al., 2023b, ApJ, 953, L21

Chen S.-R., Schive H.-Y., Chiueh T., 2017, MNRAS, 468, 1338

Chiti A., Simon J. D., Frebel A., Pace A. B., Ji A. P., Li T. S., 2022, ApJ, 939, 41

Chiti A., et al., 2023, AJ, 165, 55

Circiello A., McDaniel A., Drlica-Wagner A., Karwin C., Ajello M., Di Mauro M., Sánchez-Conde M., 2024, arXiv e-prints, p. arXiv:2404.01181

Collins M. L. M., Read J. I., 2022, Nature Astronomy, 6, 647

Collins M. L. M., Tollerud E. J., Sand D. J., Bonaca A., Willman B., Strader J., 2017, MNRAS, 467, 573

Collins M. L. M., Charles E. J. E., Martínez-Delgado D., Monelli M., Karim N., Donatiello G., Tollerud E. J., Boschin W., 2022, MNRAS, 515, L72

Conn B. C., Jerjen H., Kim D., Schirmer M., 2018, ApJ, 852, 68

Contenta F., Gieles M., Balbinot E., Collins M. L. M., 2017, MNRAS, 466, 1741

Correa Magnus L., Vasiliev E., 2022, MNRAS, 511, 2610

Crnojević D., et al., 2014, ApJ, 795, L35

Dalal N., Kravtsov A., 2022, Phys. Rev. D, 106, 063517

³⁰ https://github.com/apace7/local_volume_database

³¹ <http://leda.univ-lyon1.fr/>

³² <http://github.com/jobovy/galpy>

Danieli S., van Dokkum P., Conroy C., Abraham R., Romanowsky A. J., 2019, *ApJ*, 874, L12

Doliva-Dolinsky A., et al., 2023, *ApJ*, 952, 72

Drlica-Wagner A., et al., 2015, *ApJ*, 813, 109

Eadie G. M., Harris W. E., Springford A., 2022, *ApJ*, 926, 162

Einasto J., Saar E., Kaasik A., Chernin A. D., 1974, *Nature*, 252, 111

Elson R. A. W., Fall S. M., Freeman K. C., 1987, *ApJ*, 323, 54

Emerick A., Bryan G. L., Mac Low M.-M., 2020, *ApJ*, 890, 155

Erkal D., Belokurov V. A., 2020, *MNRAS*, 495, 2554

Erkal D., Belokurov V. A., Parkin D. L., 2020, *MNRAS*, 498, 5574

Errani R., Peñarrubia J., Walker M. G., 2018, *MNRAS*, 481, 5073

Errani R., Navarro J. F., Smith S. E. T., McConnachie A. W., 2024a, *ApJ*, 965, 20

Errani R., Ibata R., Navarro J. F., Peñarrubia J., Walker M. G., 2024b, *ApJ*, 968, 89

Fabrizio M., et al., 2016, *ApJ*, 830, 126

Fadely R., Willman B., Geha M., Walsh S., Muñoz R. R., Jerjen H., Vargas L. C., Da Costa G. S., 2011, *AJ*, 142, 88

Fahrion K., et al., 2020, *A&A*, 634, A53

Fillingham S. P., Cooper M. C., Pace A. B., Boylan-Kolchin M., Bullock J. S., Garrison-Kimmel S., Wheeler C., 2016, *MNRAS*, 463, 1916

Finlator K., Davé R., 2008, *MNRAS*, 385, 2181

Forbes D. Á., Kroupa P., 2011, *PASA*, 28, 77

Forbes D. A., Read J. I., Gieles M., Collins M. L. M., 2018, *MNRAS*, 481, 5592

Foreman-Mackey D., 2016, *The Journal of Open Source Software*, 1, 24

Foreman-Mackey D., Hogg D. W., Lang D., Goodman J., 2013, *PASP*, 125, 306

Frebel A., Norris J. E., 2015, *ARA&A*, 53, 631

Frebel A., Simon J. D., Kirby E. N., 2014, *ApJ*, 786, 74

Fritz T. K., Battaglia G., Pawłowski M. S., Kallivayalil N., van der Marel R., Sohn S. T., Brook C., Besla G., 2018, *A&A*, 619, A103

Fu S. W., et al., 2023, *ApJ*, 958, 167

Fu S. W., et al., 2024, *ApJ*, 965, 36

Galleti S., Federici L., Bellazzini M., Fusi Pecci F., Macrina S., 2004, *A&A*, 416, 917

Garnett D. R., 2002, *ApJ*, 581, 1019

Garro E. R., et al., 2020, *A&A*, 642, L19

Garro E. R., Minniti D., Fernández-Trincado J. G., 2024, *A&A*, 687, A214

Gatto M., et al., 2021, *Research Notes of the American Astronomical Society*, 5, 159

Geringer-Sameth A., Koushiappas S. M., Walker M., 2015, *ApJ*, 801, 74

Gilmore G., Wilkinson M. I., Wyse R. F. G., Kleyna J. T., Koch A., Evans N. W., Grebel E. K., 2007, *ApJ*, 663, 948

Gran F., et al., 2022, *MNRAS*, 509, 4962

Gratton R., Bragaglia A., Carretta E., D’Orazi V., Lucatello S., Sollima A., 2019, *A&A Rev.*, 27, 8

Greif T. H., Glover S. C. O., Bromm V., Klessen R. S., 2010, *ApJ*, 716, 510

Hansen T. T., et al., 2017, *ApJ*, 838, 44

Hansen T. T., et al., 2020, *ApJ*, 897, 183

Hansen T. T., Simon J. D., Li T. S., Sharkey D., Ji A. P., Thompson I. B., Reggiani H. M., Galarza J. Y., 2024, *ApJ*, 968, 21

Hargis J. R., Willman B., Peter A. H. G., 2014, *ApJ*, 795, L13

Harrington R. G., Wilson A. G., 1950, *PASP*, 62, 118

Harris W. E., 1996, *AJ*, 112, 1487

Hayashi K., Ibe M., Kobayashi S., Nakayama Y., Shirai S., 2021, *Phys. Rev. D*, 103, 023017

Heiger M. E., et al., 2024, *ApJ*, 961, 234

Ho N., et al., 2012, *ApJ*, 758, 124

Homma D., et al., 2019, *PASJ*, 71, 94

Homma D., et al., 2024, *PASJ*, 76, 733

Hunt E. L., Reffert S., 2023, *A&A*, 673, A114

Hunt L. K., et al., 2024, *arXiv e-prints*, p. arXiv:2405.13499

Hunter J. D., 2007, *Computing In Science & Engineering*, 9, 90

Ibata R., Martin N. F., Irwin M., Chapman S., Ferguson A. M. N., Lewis G. F., McConnachie A. W., 2007, *ApJ*, 671, 1591

Irwin M. J., Bunclark P. S., Bridgeland M. T., McMahon R. G., 1990, *MNRAS*, 244, 16P

Jenkins S. A., Li T. S., Pace A. B., Ji A. P., Koposov S. E., Mutlu-Pakdil B., 2021, *ApJ*, 920, 92

Ji A. P., Frebel A., Chiti A., Simon J. D., 2016, *Nature*, 531, 610

Ji A. P., Simon J. D., Frebel A., Venn K. A., Hansen T. T., 2019, *ApJ*, 870, 83

Ji A. P., et al., 2021, *ApJ*, 921, 32

Júlio M. P., Pawłowski M. S., Tony Sohn S., Taibi S., van der Marel R. P., McGaugh S. S., 2024, *A&A*, 687, A212

Kacharov N., et al., 2017, *MNRAS*, 466, 2006

Kallivayalil N., et al., 2015, *arXiv e-prints*,

Kallivayalil N., et al., 2018, *ApJ*, 867, 19

Karachentsev I. D., Karachentseva V. E., 1999, *A&A*, 341, 355

Karachentsev I. D., Makarov D. A., 1996, *AJ*, 111, 794

Karachentsev I. D., et al., 2002, *A&A*, 389, 812

Karachentsev I. D., Kashibadze O. G., Makarov D. I., Tully R. B., 2009, *MNRAS*, 393, 1265

Karachentsev I. D., Makarov D. I., Kaisina E. I., 2013, *AJ*, 145, 101

Kim S. Y., Peter A. H. G., 2021, *arXiv e-prints*, p. arXiv:2106.09050

Kim D., Jerjen H., Milone A. P., Mackey D., Da Costa G. S., 2015, *ApJ*, 803, 63

Kim D., Jerjen H., Mackey D., Da Costa G. S., Milone A. P., 2016, *ApJ*, 820, 119

Kim S. Y., Peter A. H. G., Hargis J. R., 2018, *Phys. Rev. Lett.*, 121, 211302

King I., 1962, *AJ*, 67, 471

Kirby E. N., Lanfranchi G. A., Simon J. D., Cohen J. G., Guhathakurta P., 2011, *ApJ*, 727, 78

Kirby E. N., Boylan-Kolchin M., Cohen J. G., Geha M., Bullock J. S., Kaplinghat M., 2013a, *ApJ*, 770, 16

Kirby E. N., Cohen J. G., Guhathakurta P., Cheng L., Bullock J. S., Gallazzi A., 2013b, *ApJ*, 779, 102

Kirby E. N., Bullock J. S., Boylan-Kolchin M., Kaplinghat M., Cohen J. G., 2014, *MNRAS*, 439, 1015

Kirby E. N., Cohen J. G., Simon J. D., Guhathakurta P., Thygesen A. O., Duggan G. E., 2017, *ApJ*, 838, 83

Klypin A., Kravtsov A. V., Valenzuela O., Prada F., 1999, *ApJ*, 522, 82

Koposov S., et al., 2007, *ApJ*, 669, 337

Koposov S., et al., 2008, *ApJ*, 686, 279

Koposov S. E., et al., 2015, *ApJ*, 811, 62

Kravtsov A., Manwadkar V., 2022, *MNRAS*, 514, 2667

Kruijssen J. M. D., Pfeffer J. L., Reina-Campos M., Crain R. A., Bastian N., 2019, *MNRAS*, 486, 3180

Kunder A., Crabb R. E., Debattista V. P., Koch-Hansen A. J., Huhmann B. M., 2021, *AJ*, 162, 86

Laevens B. P. M., et al., 2014, *ApJ*, 786, L3

Laevens B. P. M., et al., 2015, *ApJ*, 813, 44

Larsen S. S., Romanowsky A. J., Brodie J. P., Wasserman A., 2020, *Science*, 370, 970

Li T. S., et al., 2018, *ApJ*, 866, 22

Libralato M., et al., 2022, *ApJ*, 934, 150

Longeard N., Martin N., Ibata R. A., Collins M. L. M., Laevens B. P. M., Bell E., Mackey D., 2019, *MNRAS*, 490, 1498

Longeard N., et al., 2021, *MNRAS*, 503, 2754

Lynden-Bell D., 1976, *MNRAS*, 174, 695

Lynden-Bell D., 1981, *The Observatory*, 101, 111

Makarov D., Prugniel P., Terekhova N., Courtois H., Vauglin I., 2014, *A&A*, 570, A13

Manwadkar V., Kravtsov A. V., 2022, *MNRAS*, 516, 3944

Marshall J. L., et al., 2019, *ApJ*, 882, 177

Martin N. F., Ibata R. A., Irwin M. J., Chapman S., Lewis G. F., Ferguson A. M. N., Tanvir N., McConnachie A. W., 2006, *MNRAS*, 371, 1983

Martin N. F., Ibata R. A., Chapman S. C., Irwin M., Lewis G. F., 2007, *MNRAS*, 380, 281

Martin N. F., et al., 2013a, *ApJ*, 772, 15

Martin N. F., et al., 2013b, *ApJ*, 779, L10

Martin N. F., et al., 2016, *ApJ*, 830, L10

Martin N. F., et al., 2022, *Nature*, 601, 45

Martínez-Delgado D., Karim N., Charles E. J. E., Boschin W., Monelli M., Collins M. L. M., Donatiello G., Alfaro E. J., 2022, *MNRAS*, 509, 16

Martínez-Delgado D., Stein M., Pawłowski M. S., Makarov D., Makarova L., Donatiello G., Lang D., 2024, *arXiv e-prints*, p. arXiv:2405.03769

Massari D., Breddels M. A., Helmi A., Posti L., Brown A. G. A., Tolstoy E., 2018, *Nature Astronomy*, 2, 156

Massari D., Koppelman H. H., Helmi A., 2019, *A&A*, 630, L4

Mateu C., 2023, *MNRAS*, 520, 5225

Mau S., et al., 2020, *ApJ*, 890, 136

McConnachie A. W., 2012, *AJ*, 144, 4

McConnachie A. W., Côté P., 2010, *ApJ*, 722, L209

McConnachie A. W., Venn K. A., 2020, *AJ*, 160, 124

McConnachie A. W., Higgs C. R., Thomas G. F., Venn K. A., Côté P., Battaglia G., Lewis G. F., 2021, *MNRAS*, 501, 2363

McDaniel A., Ajello M., Karwin C. M., Di Mauro M., Drlica-Wagner A., Sánchez-Conde M. A., 2024, *Phys. Rev. D*, 109, 063024

McQuinn K. B. W., Mao Y.-Y., Buckley M. R., Shih D., Cohen R. E., Dolphin A. E., 2023, *ApJ*, 944, 14

McQuinn K. B. W., Mao Y.-Y., Tollerud E. J., Cohen R. E., Shih D., Buckley M. R., Dolphin A. E., 2024, *ApJ*, 967, 161

Minniti D., et al., 2011, *A&A*, 527, A81

Minor Q. E., Martinez G., Bullock J., Kaplinghat M., Trainor R., 2010, *ApJ*, 721, 1142

Minor Q. E., Pace A. B., Marshall J. L., Strigari L. E., 2019, *MNRAS*, 487, 2961

Moore B., Ghigna S., Governato F., Lake G., Quinn T., Stadel J., Tozzi P., 1999, *ApJ*, 524, L19

Muñoz R. R., Geha M., Côté P., Vargas L. C., Santana F. A., Stetson P., Simon J. D., Djorgovski S. G., 2012, *ApJ*, 753, L15

Muñoz R. R., Côté P., Santana F. A., Geha M., Simon J. D., Oyarzún G. A., Stetson P. B., Djorgovski S. G., 2018, *ApJ*, 860, 66

Müller O., Jerjen H., Binggeli B., 2017, *A&A*, 597, A7

Müller O., et al., 2021, *A&A*, 645, A92

Mutlu-Pakdil B., et al., 2021, *ApJ*, 918, 88

Mutlu-Pakdil B., et al., 2024, *ApJ*, 966, 188

Nadler E. O., et al., 2020, *ApJ*, 893, 48

Nadler E. O., et al., 2021, *Phys. Rev. Lett.*, 126, 091101

Nadler E. O., Gluscevic V., Driskell T., Wechsler R. H., Moustakas L. A., Benson A., Mao Y.-Y., 2024, *ApJ*, 967, 61

Newton O., Cautun M., Jenkins A., Frenk C. S., Helly J. C., 2018, *MNRAS*, 479, 2853

Nidever D. L., et al., 2024, in Tabatabaei F., Barbuy B., Ting Y.-S., eds, IAU Symposium Vol. 377, Early Disk-Galaxy Formation from JWST to the Milky Way, pp 115–122 (arXiv:2306.04688), doi:10.1017/S1743921323002016

Oh S.-H., et al., 2015, *AJ*, 149, 180

Ou X., et al., 2024, *ApJ*, 966, 33

Pace A. B., Strigari L. E., 2019, *MNRAS*, 482, 3480

Pace A. B., et al., 2020, *MNRAS*, 495, 3022

Pace A. B., Erkal D., Li T. S., 2022, *ApJ*, 940, 136

Pace A. B., et al., 2023, *MNRAS*, 526, 1075

Patel E., Mandel K. S., 2023, *ApJ*, 948, 104

Patel E., Besla G., Sohn S. T., 2017, *MNRAS*, 464, 3825

Patel E., et al., 2020, *ApJ*, 893, 121

Pawlowski M. S., 2021, *Galaxies*, 9, 66

Pawlowski M. S., Kroupa P., 2020, *MNRAS*, 491, 3042

Peñarrubia J., Ma Y.-Z., Walker M. G., McConnachie A., 2014, *MNRAS*, 443, 2204

Pérez F., Granger B. E., 2007, *Computing in Science and Engineering*, 9, 21

Plummer H. C., 1911, *MNRAS*, 71, 460

Price-Whelan A. M., 2017, *The Journal of Open Source Software*, 2

Richardson J. C., et al., 2011, *ApJ*, 732, 76

Richstein H., et al., 2024, *ApJ*, 967, 72

Roederer I. U., et al., 2016, *AJ*, 151, 82

Sand D. J., et al., 2014, *ApJ*, 793, L7

Sand D. J., et al., 2022, *ApJ*, 935, L17

Sérsic J. L., 1968, *Atlas de Galaxias Australes*

Shapley H., 1938, *Nature*, 142, 715

Simon J. D., 2018, *ApJ*, 863, 89

Simon J. D., 2019, *ARA&A*, 57, 375

Simon J. D., Geha M., 2007, *ApJ*, 670, 313

Simon J. D., et al., 2011, *ApJ*, 733, 46

Simon J. D., et al., 2017, *ApJ*, 838, 11

Simon J. D., et al., 2024, arXiv e-prints, p. arXiv:2410.08276

Smith S. E. T., et al., 2023, *AJ*, 166, 76

Smith S. E. T., et al., 2024, *ApJ*, 961, 92

Sohn S. T., Patel E., Fardal M. A., Besla G., van der Marel R. P., Geha M., Guhathakurta P., 2020, *ApJ*, 901, 43

Spitler L. R., Forbes D. A., 2009, *MNRAS*, 392, L1

Strigari L. E., 2018, *Reports on Progress in Physics*, 81, 056901

Taibi S., Battaglia G., Leaman R., Brooks A., Riggs C., Munshi F., Revaz Y., Jablonka P., 2022, *A&A*, 665, A92

Tollerud E. J., Bullock J. S., Strigari L. E., Willman B., 2008, *ApJ*, 688, 277

Tolstoy E., Hill V., Tosi M., 2009, *ARA&A*, 47, 371

Tolstoy E., et al., 2023, *A&A*, 675, A49

Torreala G., Koposov S. E., Belokurov V., Irwin M., 2016, *MNRAS*, 459, 2370

Torreala G., et al., 2018, *MNRAS*, 475, 5085

Tulin S., Yu H.-B., 2018, *Phys. Rep.*, 730, 1

Tully R. B., Rizzi L., Shaya E. J., Courtois H. M., Makarov D. I., Jacobs B. A., 2009, *AJ*, 138, 323

Valli M., Yu H.-B., 2018, *Nature Astronomy*, 2, 907

Vasiliev E., 2023, *Galaxies*, 11, 59

Vasiliev E., Baumgardt H., 2021, *MNRAS*, 505, 5978

Virtanen P., et al., 2020, *Nature Methods*, 17, 261

Vitral E., et al., 2024, *ApJ*, 970, 1

Walker M. G., Mateo M., Olszewski E. W., Gnedin O. Y., Wang X., Sen B., Woodroofe M., 2007, *ApJ*, 667, L53

Walker M. G., Mateo M., Olszewski E. W., 2009a, *AJ*, 137, 3100

Walker M. G., Mateo M., Olszewski E. W., Peñarrubia J., Wyn Evans N., Gilmore G., 2009b, *ApJ*, 704, 1274

Walker M. G., Caldwell N., Mateo M., Olszewski E. W., Pace A. B., Bailey J. I., Koposov S. E., Roederer I. U., 2023, *ApJS*, 268, 19

Walsh S. M., Jerjen H., Willman B., 2007, *ApJ*, 662, L83

Walt S. v. d., Colbert S. C., Varoquaux G., 2011, *Computing in Science & Engineering*, 13, 22

Wan Z., et al., 2020, *Nature*, 583, 768

Warfield J. T., et al., 2023, *MNRAS*, 519, 1189

Weatherford N. C., Chatterjee S., Rodriguez C. L., Rasio F. A., 2018, *ApJ*, 864, 13

Weatherford N. C., Chatterjee S., Kremer K., Rasio F. A., 2020, *ApJ*, 898, 162

Webb J. J., Carlberg R. G., 2021, *MNRAS*, 502, 4547

Weerasooriya S., Bovill M. S., Taylor M. A., Benson A. J., Leahy C., 2024, *ApJ*, 968, 78

Weiner B. J., et al., 2006, *ApJ*, 653, 1027

Weisz D. R., et al., 2016, *ApJ*, 822, 32

Willman B., Strader J., 2012, *AJ*, 144, 76

Willman B., et al., 2005, *AJ*, 129, 2692

Willman B., Geha M., Strader J., Strigari L. E., Simon J. D., Kirby E., Ho N., Warrens A., 2011, *AJ*, 142, 128

Wolf J., Martinez G. D., Bullock J. S., Kaplinghat M., Geha M., Muñoz R. R., Simon J. D., Avedo F. P., 2010, *MNRAS*, 406, 1220

Zucker D. B., et al., 2004, *ApJ*, 612, L121

van den Bergh S., 1972, *ApJ*, 171, L31

van der Marel R. P., Guhathakurta P., 2008, *ApJ*, 678, 187

van der Marel R. P., et al., 2014, in Seigar M. S., Treuthardt P., eds, *Astronomical Society of the Pacific Conference Series* Vol. 480, *Structure and Dynamics of Disk Galaxies*, p. 43 (arXiv:1309.2014), doi:10.48550/arXiv.1309.2014

keys required for each system. The detailed description of each YAML key are as follows:

- **key** (required)—the unique internal identifier a system in the LVDB, this also corresponds to the name of the YAML file. All LVDB **key**'s are lower case and most distant systems are grouped (for example, Cen A satellites start with `cen_a_` and the LMC globular clusters start with `lmc_gc_`).
- **table** (required)—the table to place the system in the combined catalogs.
- **location** (required)—Collection with YAML keys: `ra` and `dec`. Location of system [degrees, ICRS frame, J2000.0].
- **name_discovery**—Collection on discovery and classification information.
 - **name**: Name of the system.

- `other_name`: List of additional names of the system.
- `ref_discovery`: List of discovery reference(s). Multiple references are allowed to account for simultaneous discoveries, re-discovery, confirmation, and/or classification changes.
- `discovery_year`: The year of discovery.
- `host`: Host galaxy of the system.
- `confirmed_dwarf`: Dwarf galaxy classification column. 1 corresponds to dwarf galaxy classification. See Section 2.2.2 for details on the classification.
- `confirmed_star_cluster`: Star cluster classification column. 1 corresponds to a star cluster classification. See Section 2.2.2 for details on the classification.
- `confirmed_real`: Denotes whether the system should be considered a candidate ($=0$) or whether the system has been confirmed ($=1$). Confirmation may occur with deeper photometric imaging, astrometry, and/or spectroscopy. For distant dwarf galaxies ($d \gtrsim 3$ Mpc) this generally requires space based imaging.
- `false_positive`: Denotes whether system is a false positive ($=1$; chance alignment or artifact) or background galaxy ($=2$).
- `ref_false_positive`: Reference(s) that confirm the system is a false positive or background galaxy.
- `type`: Type of galaxy or star cluster (e.g., dSph, dIrr, dE, GC, SC, NSC etc).
- `abbreviation`: Short 3-5 character abbreviation for the system.

- `structure`—Collection of structural parameters.
- `rhalf`: Projected (2D) half-light radius along the major axis of the system in angular units. The units are specified in the `spatial_unit` key. If the `spatial_unit` is not included, the default units are arcmin.
- `spatial_unit`: Input spatial units of the `rhalf` column [options = arcmin or arcsec].
- `ellipticity`: Ellipticity of the system, defined as, $\epsilon = 1 - b/a$, where b and a are the minor and major axis, respectively.
- `position_angle`: Position angle of the system, defined as the angle from North to East.
- `ref_structure`: Reference.

- `distance`—Distance collection.
- `distance_modulus`: Distance modulus.
- `distance_fixed_host`: When this option is set (`=true`), the distance to the system is fixed to its host.
- `ref_distance`: Reference.

- `m_v`—Apparent magnitude collection.
- `apparent_magnitude_v`: Apparent magnitude in the V-band corrected for extinction.
- `mean_ebv`: Mean E(B-V) reddening.
- `ref_m_v`: Reference.

- `velocity`—Stellar kinematic collection.
- `vlos_systemic`: Systemic heliocentric (line-of-sight) velocity of the system [km s $^{-1}$].
- `vlos_sigma`: Global line-of-sight velocity dispersion [km s $^{-1}$].
- `vlos_sigma_central`: Central velocity dispersion [km s $^{-1}$]. Generally used for globular clusters.
- `vlos_rotation`: Stellar rotation [km s $^{-1}$].
- `ref_vlos`: Reference.

- `proper_motion`—Systemic proper motion collection.
- `pmra`: Systemic proper motion in right ascension [mas yr $^{-1}$]. Includes $\cos \delta$ term.
- `pmdec`: Systemic proper motion in declination [mas yr $^{-1}$].
- `ref_proper_motion`: Reference.

- `spectroscopic_metallicity`—Stellar spectroscopic metallicity collection.
- `metallicity_spectroscopic`: Mean spectroscopic metallicity ([Fe/H]).
- `metallicity_spectroscopic_sigma`: Spectroscopic metallicity dispersion.
- `ref_metallicity_spectroscopic`: Reference.

- `photometric_metallicity`—Photometric metallicity collection.
- `metallicity_photometric`: Metallicity measured from photometric studies (e.g., metallicity sensitive photometry).
- `metallicity_photometric_sigma`: Metallicity dispersion from photometric based measurements.
- `ref_metallicity_photometric`: Reference.

- `metallicity_isochrone`—Photometric metallicity collection.
- `metallicity_isochrone`: Metallicity measured from isochrone or color-magnitude diagram.
- `metallicity_isochrone_sigma`: Metallicity dispersion from isochrone or color-magnitude diagram based measurements
- `ref_metallicity_isochrone`: Reference.

- `structure_king`—King stellar profile collection. (King 1962).

- `rcore`: King core radius.
- `rking`: King limiting radius. Commonly referred to as the tidal radius.
- `spatial_unit`: Spatial units [arcmin or arcsec] of `rcore` and `rking`.
- `ellipticity`: Ellipticity from King profile fit.
- `position_angle`: Position angle from King profile fit.
- `ref_king`: Reference.
- `structure_sersic`—Sersic spatial profile collection (Sérsic 1968).
 - `n_sersic`: Sersic power-law index.
 - `rad_sersic`: Sersic scale radius.
 - `spatial_unit`: Spatial units [arcmin or arcsec] of `rad_sersic`.
 - `ellipticity`: Ellipticity from Sersic profile fit.
 - `position_angle`: Position angle from Sersic profile fit.
 - `ref_sersic`: Reference.
- `structure_eff`—EFF spatial profile collection (Elson et al. 1987).
 - `gamma_eff`: EFF power-law index.
 - `rad_eff`: EFF scale radius.
 - `spatial_unit`: Spatial units [arcmin or arcsec] of `rad_eff`.
 - `ellipticity`: Ellipticity from EFF profile fit.
 - `position_angle`: Position angle from EFF profile fit.
 - `ref_eff`: Reference.
- `structure_plummer`—Plummer spatial profile collection (Plummer 1911).
 - `rplummer`: Plummer profile scale radius.
 - `spatial_unit`: Spatial units [arcmin or arcsec] of `rplummer`.
 - `ellipticity`: Ellipticity from Plummer profile fit.
 - `position_angle`: Position angle from Plummer profile fit.
 - `ref_plummer`: Reference.
- `structure_exponential`—Exponential spatial profile collection.
 - `r_exponential`: Exponential scale radius.
 - `spatial_unit`: Spatial units [arcmin or arcsec] of `r_exponential`.
 - `ellipticity`: Ellipticity from Exponential profile fit.
 - `position_angle`: Position angle from Exponential profile fit.
 - `ref_eff`: Reference.
- `age`—Age collection.
 - `age`: Mean age of system [Gyr] for single stellar population systems (i.e., star clusters)
 - `ref_age`: Reference.
- `flux_HI`—Gas (HI) collection.
 - `flux_HI`: HI flux of system [Jy km s⁻¹].
 - `vlos_systemic_HI`: Systemic velocity of HI gas in system [km s⁻¹].
 - `sigma_HI`: Velocity dispersion of HI gas [km s⁻¹].
 - `vrot_HI`: Rotation velocity of HI gas [km s⁻¹].
 - `ref_flux_HI`: Reference.
- `star_formation_history`: Star formation history collection. Galaxy focused.
 - `tau_50`: Time for 50 per cent of stellar mass to form [Gyr]. Median age of system.
 - `tau_80`: Time for 80 per cent of stellar mass to form [Gyr]. Quenching Time.
 - `tau_90`: Time for 90 per cent of stellar mass to form [Gyr]. Quenching Time.
 - `ref_star_formation_history`: Reference.
- `notes`—Miscellaneous notes about the system. This may include details about measurements in the LVDB YAML file or details about the classification of the system. The notes vary significantly from system to system.

For systems without a particular measurement, the corresponding YAML key is not included and the parameters will be empty in the combined catalog. For all measured parameters there can be error keys. The errors keys are column name + (`_em`, `_ep`, `_ul`, `_ll`). The error names correspond to: `_em`—16% confidence/credible interval (error minus; i.e., minus one sigma); `_ep`—84% confidence/credible interval (error plus; i.e., plus one sigma); `_ul`—95.5% confidence/credible interval (upper limit, i.e. two sigma upper limit), generally used as an upper limit; `_ll`—4.5% confidence/credible interval (lower limit, i.e. two sigma lower limit), generally used as an lower limit. For some entries (generally, the velocity or metallicity dispersion), I have reanalyzed data sets to quote consistent upper limits. However, even with this reanalysis some limits are quoted at different values³³. When this occurs, this detail are included in the `notes` key.

The `ref` keys follow a consistent schema of author last name + ADS bibcode. The author's last name is stripped of special characters and spaces but capitalization is kept. While the ADS bibcode is a unique identifier for a reference, the addition of the author's last name significantly improves the human interpretability of the LVDB reference columns. To aid in enabling references to the internal contents of the database, there is an up-to-date BibTeX file containing all entries in the LVDB with the

³³ The most common measurement with different limits are HI flux limits. These vary from 2-5 σ in the literature.

LVDB `ref` schema³⁴ and I have made an ADS library that includes the LVDB references³⁵. As the ADS bibcode has a fixed length of 19 characters, the ADS bibcode can be derived from the last 19 characters of the LVDB `ref` columns.

For many systems, there may be a number of different studies of the same measurement or property (i.e. distance, half-light radius etc) and the decision of which measurement to include is subjective. The sample size, depth, field-of-view, precision, and methodology are considered when deciding on which measurement to include. I note that many YAML keys were added after the creation of the LVDB and many newer entries are incomplete (this includes `mean_ebv`, `type`, HI kinematics, `star_formation_history`).

There are some fundamental dwarf galaxy and star cluster properties that I have opted not to include. These quantities are generally model dependent. One example are the orbital properties (e.g., pericenter and apocenter) of dwarf galaxies and star clusters. The orbital properties are highly dependent on the MW potential assumed, whether the influence of the LMC was included in the orbit calculations, the input parameters (which may differ from the values here), and the choice of solar motion. While I include the dynamical mass within the half-light radius as a value-added quantity, I have not included any mass or density measurements from detailed dynamical modeling.

A.1. Value-Added Columns

The combined catalogs have additional value-added columns and these include:

- `M_V`—Absolute magnitude in the V-band (M_V). Computed from the apparent magnitude and distance modulus. Note that the distance errors are commonly not included when computing the the absolute magnitude and I follow that convention here.
- `mass_stellar`—Stellar mass computed from M_V assuming a mass-to-light ratio of 2 [$\log_{10} M_\odot$].
- `distance`—Heliocentric distance to the system, computed from the distance modulus [kpc].
- `ll, bb`—Location of the system in Galactic coordinates [degree, degree].
- `sg_xx, sg_yy, sg_zz`—Cartesian coordinates of the system in Supergalactic coordinates [kpc, kpc, kpc].
- `distance_gc, distance_m31, distance_lg, distance_host`—Distance of the system relative to the Galactic center, M31, the Local Group center, and the system's host galaxy, respectively [kpc, kpc, kpc, kpc].
- `rhalf_physical`—Major-axis of half-light radius in physical units [parsec]. This column includes errors from a Monte Carlo sampling of the half-light radius and distance errors.

³⁴ Link to BibTeX file

³⁵ Link to ADS library

- `rhalf_sph_physical`—azimuthally-averaged half-light radius (also referred to as the geometric mean) in physical units [parsec]. This column includes errors from a Monte Carlo sampling of the half-light radius, ellipticity, and distance errors.
- `surface_brightness_rhalf`—Average surface brightness enclosed within the azimuthally-averaged half-light radius [mag arcsec $^{-2}$].
- `mass_HI`—HI (gas) mass. The HI mass is computed from $M_{HI} = 2.356 \times 10^5 (d/\text{Mpc})^2 S$, where S is the HI flux and d is the distance in Mpc [$\log_{10} M_\odot$].
- `metallicity`—Combined metallicity column. The order of preference is: spectroscopic, photometric, and isochrone.
- `metallicity_type`—Metallicity type (spectroscopic, photometric, isochrone) of `metallicity` column.
- `velocity_gsr`—Velocity in the Galactic standard of rest [km s $^{-1}$].
- `velocity_lg`—Velocity relative to the Local Group [km s $^{-1}$]
- `mass_dynamical_wolf`—Dynamical mass using the Wolf et al. (2010) mass estimator for a pressure-supported system ($M(r = r_{1/2}) = 930 \sigma^2 R_{1/2}$). This column includes errors from a Monte Carlo sampling of the velocity dispersion, half-light radius, ellipticity, and distance errors [$\log_{10} M_\odot$].

B. SECONDARY COMPILATIONS

The primary catalogs in the LVDB only include a single entry per property. There are two additional catalogs that are included as compilations of literature measurements.

B.1. Systemic Proper Motion of Dwarf Galaxies

I include a compilation of systemic proper motion measurements of dwarf galaxies and some HFCSS³⁶. This catalog was created for literature comparison in the Pace et al. (2022) analysis³⁷ and subsequently updated. This includes ground, space based (e.g., *HST*), and *Gaia* measurements. Each entry in the catalog contains: LVDB key, LVDB reference, ADS bibcode, systemic proper motion measurement ($\mu_{\alpha*}, \mu_\delta$, including the correlation and asymmetric errors), text citation (e.g., Pace et al. 2022 or Simon 2020), method (*Gaia*, *HST*, etc), and comments. There is an example notebook³⁸ in the GitHub repository that describes the use of this catalog and creates comparison figures of systemic proper motion measurements for a system. These plots are similar to comparison plots in Pace et al. (2022) and can be used to compare new measurements to the literature. This compilation is complete for MW dwarf galaxies and only contains published measurements.

³⁶ Link to the proper motion compilation.

³⁷ The comparison figures are only included in the arXiv/preprint version of Pace et al. (2022).

³⁸ Link to example proper motion notebook.

B.2. Astrophysical J-factors for the Indirect Detection of Dark Matter

I include a compilation of astrophysical J-factors of MW dwarf galaxies for studies of the indirect detection of dark matter³⁹. The J-factor is the astrophysical component of the dark matter annihilation flux. There are a number of J-factors analyses focusing on the MW dwarf galaxies (e.g., Geringer-Sameth et al. 2015; Bonnivard et al. 2015; Pace & Strigari 2019). Similar to the proper motion compilation, this is a compilation of measurements and includes multiple measurements per galaxy. Each entry in the catalog contains: LVDB key, LVDB reference, ADS bibcode, text citation, selection (i.e., methodology grouping), angle [degree], J-factor measurement [$(\log_{10} J)$ (this includes median, one and two sigma asymmetric errors and an upper limit column), use (another selection type column), and comments. I include this compilation primarily to compare new J-factor measurements to literature results and in many analyses, utilizing a consistent J-factor analysis is ideal. Unlike the proper motion compilation, the J-factor compilation is quite incomplete of literature analyses. There is an example notebook⁴⁰ in the GitHub repository that describes the use of this catalog and creates some summary figures.

C. SUMMARY TABLES

In addition to data catalogs, there is a pdf document with summary tables of the LVDB content. These tables are created via python and LaTeX scripts from the LVDB catalogs and YAML files and the summary file is included as part of the GitHub release⁴¹. Each primary catalog has four tables and the content of table each is described below.

The first table is focused on the discovery and classification of each system. The columns are as follows: (1) System name. (2) Other names for system. (3) RA (hms). (4) Dec (dms). (5) Host Galaxy. (6) Discovery reference(s). (7) Denotes whether system is confirmed or a candidate. (8) Type/classification of the system. This includes both dwarf galaxy (dSph, dIrr, etc) and star cluster types (star cluster (SC), nuclear star cluster (NSC), globular cluster (GC)). This table is sorted by discovery year and then LVDB key. For the dwarf galaxy hosted globular clusters and Local Volume dwarf galaxy tables, the systems are first sorted by host LVDB

key.

The second table is focused on the structural parameters, distance, and luminosity. The columns are as follows: (1) System name. (2) RA (deg). (3) Dec (deg). (4) Half-light radius along the major axis. (5) Ellipticity. (6) Position angle. (7) Azimuthally-averaged half-light radius in physical units. (8) Distance modulus. (9) Distance. (10) Extinction corrected apparent V-band magnitude. (11) Extinction corrected absolute V-band magnitude. (12) References. This table and the following tables are sorted by the LVDB key. For the dwarf galaxy hosted globular cluster and Local Volume dwarf galaxy tables, this table and the following tables are first sorted by host LVDB key then system LVDB key.

The third table is focused on the systemic motion, (stellar) kinematics, and (spectroscopic) metallicity. The columns are as follows: (1) System name. (2) Galactic longitude (deg). (3) Galactic latitude (deg). (4) Systemic (line-of-sight) velocity. (5) Global velocity dispersion. (6) Spectroscopic stellar mean metallicity. (7) Spectroscopic metallicity dispersion. (8) Systemic proper motion in the direction of right ascension. (9) Systemic proper motion in the direction of declination. (10) References. For globular cluster tables, an additional age column is added after the spectroscopic metallicity dispersion column.

The fourth table is focused on the stellar mass, dynamical mass, and HI gas mass. The columns are as follows: (1) System name. (2) Stellar mass assuming a mass-to-light ratio of 2. (3) Dynamical mass within the 3D half-light radius from stellar kinematics. (4) Dynamical mass-to-light ratio within the half-light radius from stellar kinematics. (5) HI gas mass. (6) Ratio of HI-to-stellar mass. (7) References. This table is not included for the globular clusters catalogs.

Lastly, there are two tables for low significance candidates, false positive, and background galaxy systems. The first table is similar to the previous discovery tables with the candidate column is replaced by a description of why the system is included in this catalog. This includes: candidate (Cand.), known false positive (FP), or background galaxy (BG). The type column is replaced with references to the false positive classification. The second table is similar to the structural parameter table, however, I omit errors and add the Galactic longitude and latitude.

³⁹ Link to J-factor compilation.

⁴⁰ Link to example J-factor notebook.

⁴¹ Named `1vdb_table.pdf` on the GitHub release pages (Link).